Slow light enhancement and limitations in periodic media

Grgic, Jure

Publication date:
2012

Document Version
Publisher's PDF, also known as Version of record

Slow light enhancement and limitations in periodic media

Jure Grgić

Supervisors:
Prof. N. Asger Mortensen,
Prof. Jesper Mørk and
Prof. Antti–Pekka Jauho

DTU Fotonik
Department of Photonics Engineering
Technical University of Denmark
Building 343
2800 Kgs. Lyngby
Denmark

I dedicate this thesis to my
mother Lena. To whom I owe
all achievements in my life.

Abstract

Properties of periodic dielectric media have attracted a big interest in the last two decades due to numerous exciting physical phenomena that cannot occur in homogeneous media. Due to their strong dispersive properties, the speed of light can be significantly slowed down in periodic structures. When light velocity is much smaller than the speed of light in a vacuum, we describe this phenomena as slow light. In this thesis, we analyze important properties of slow light enhancement and limitations in periodic structures. We analyze quantitatively and qualitatively different technologies and significant structures with numerical and analytical methods. By analyzing different structures, we show very general properties for limitation and enhancement in the slow light regime.

Inherent imperfections of fabricated structures such as a material loss and structural disorder have a strong influence on slowly propagating light. By means of perturbative analysis, we address the effect of small imperfections in periodic structures. From our analysis, we find very universal behavior in a slow light regime for all periodic structures. Even if losses are very small the dispersion is severely affected in the vicinity of the band edge. The minimum attainable group velocity will depend on the amount of imperfections. Since imperfections are inherited as part of any periodic structure it is necessary to take them into account when we are interested in slow light applications.

Slowly propagating light gives rise to longer interaction time in the periodic media. Due to this reason, weak light-matter interaction is enhanced. The enhancement due to slow light has been studied for loss and gain. By introducing gain/loss, dispersive properties, in the slow light region, are severely influenced. The minimum attainable group velocity is strongly dependent on the amount of introduced loss/gain that will result in limitation of enhancement. Therefore, small amounts of gain/loss will provide great enhancement. While for a large amount of gain/loss slow, light is heavily jeopardized, hence no enhancement will occur.

Resumé

Egenskaberne af periodiske dielektriske materialer har tiltrukket sig stor interesse i de seneste to årtier påbaggrund af et stort antal fysiske fænomener, der ikke kan finde sted i homogene materialer. Lysets hastighed kan blive sænket betydeligt på grund af den stærke dispersion der kan opnås. Når lysets hastighed bliver meget mindre en lysets hastighed i vakuum, beskriver vi dette fænomen som langsomt lys. I denne afhandling analyserer vi vigtige egenskaber af forstærkning og begrænsning ved langsomt lys. Vi analyserer kvantitativt og kvalitativt de vigtige strukturer indenfor forskellige teknologier ved hjælp af numeriske og analytiske metoder. Ved analyse af forskellige strukturer vises meget generelle egenskaber for begrænsning og forstærkning i regimet med langsomt lys.

Fabrikerede strukturers medfødte defekter, såsom tab og strukturel uorden, har stor indflydelse på egenskaberne af langsomt propagerende lys. Ved hjælp af perturbations analyse, beskrives effekten af små defekter i periodiske strukturer. Analysen viser en meget generel opførsel i et regime med langsomt lys for alle periodiske strukturer. Selv hvis tabene er meget små vil dispersionen blive betydeligt påvirket i omegnen af båndkanten. Den mindste opnåelige gruppehastighed vil afhænge af antallet af defekter. Da defekter er medfødte i alle periodisk strukturer, er det nødvendigt at de inkluderes når vi er interesserede i anvendelser af langsomt lys.

Langsomt propagerende lys giver anledning til længere tids vekselvirkning i det periodiske medium. Af denne grund bliver svag vekselvirkning mellem lys og materiale forstærket. Denne forstærkning på grund af langsomt lys er blevet studeret i tilfælde med både tab og forstærkning. Når tab/forstærkning introduceres bliver dispersionen i regimet med langsom lys kraftigt påvirket. Den mindste opnåelige gruppehastighed er stærkt afhængig af mængden af tab/forstærkning, hvilket vil resultere i begrænsning af effekten. Derfor vil små tab/forstærkning give en stærk effekt. For stort tab/forstærkning bliver langsomt lys stærkt begrænset, hvorved ingen forstærkning vil finde sted.

Preface and Acknowledgments

This thesis is submitted in partial fulfillment of the requirements for obtaining the Doctor of Philosophy (Ph.D) degree at the Technical University of Denmark (DTU). The work presented here has been carried out at the Department of Photonics engineering (DTU Fotonik) in Structured Electromagnetic Group. The work presented in this Thesis was carried out between January 2009 and March 2012. My project was supervised by Prof. N Asger Mortensen, Prof. Jesper Mørk and Prof. Antti–Pekka Jauho and financed by VKR Center of excellence NATEC.

My experience as PhD student in DTU Fotonik has been a really nice journey. I learned a lot, I met plenty of nice people, I have heard many interesting talks, seminars, lectures and have the privilege to work with a lot of great scientists and researchers. First, I would like to acknowledge and express my gratitude to my main supervisor N. Asger Mortensen for encouragement, inspiring discussion, guidance and keeping me always motivated during my PhD. I am profoundly thankful to Jesper Mørk for all fruitful discussion and invaluable help. I would like to thank Antti–Pekka Jauho for many helpful discussions and suggestion. I would like to thank Alfredo De Rossi, Morten Willatzen and Andrei Lavrinenko for serving on the evaluation committee of my thesis.

It was a real pleasure to be a part of "Structured Electromagnetic Materials" group, and I would like to than all my colleagues. In particular, big thanks go to Marijn Wubs and Sanshui Xiao for discussing and helping me in all phases of PhD. There is a long list of colleagues to whom I am very thankful for all nice discussion and help in these three years of my PhD: Min Yan, Niels Gregersen, Torben R. Nilsen, Fengweng Wang, Ole Sigmund, Fabrizio Frezza, Paolo Bassi, Philp Trost, Yahoui Chen, and Jesper G. Pedersen.It has been great pleasure to share office with Søren Raza, Jeppe Claussen and Johan R. Ott. Thanks guys for keeping always good and pleasant working atmosphere. Special thank goes to my dear fiend and colleague Johan for

plenty of good discussions, reading of my thesis and all non-scientifical . I would like to thank Kamau for reading my thesis. I would like to thank all my friends but in particular, Darko and Marko.

Last but not least big love and thanks to a whole my family that was always with me in all difficult and happy moments of my life.

Jure Grgić
March 2012

List of publications

Journal Publications

[A] **J. Grgić**, J. G. Pedersen, S. Xiao and N. A. Mortensen, "Group-index limitations in slow-light photonic crystals", Photonics Nanostruct. **8**, 56–61 (2010).

[B] S. Raza, **J. Grgić**, J. G. Pedersen, S. Xiao and N. A. Mortensen, "Coupled-resonator optical waveguides: Q-factor influence on slow-light propagation and the maximal group delay", J. Eur. Opt. Soc. Rap. Publ. **5**, 10009 (2010).

[C] **J. Grgić**, E. Campagnoli, S. Raza, P. Bassi and N. A. Mortensen, "Coupled-resonator optical waveguides: Q-factor and disorder influence", Opt. Quant. Electron. **42**, 511 (2011).

[D] **J. Grgić** , S. Xiao, J. Mørk, A.-P. Jauho and N. A. Mortensen, "Slow-light enhanced absorption in a hollow-core fiber", Opt. Express **118**, 14270–14279, (2010).

[E] **J. Grgić**, J. R. Ott, F. Wang, O. Sigmund, A.-P. Jauho, J. Mørk, and N. A. Mortensen, "Fundamental limits to gain enhancement in periodic media and waveguides", Phys. Rev. Lett. **108**, 183903 (2012).

Contents

1

Introduction

There are various reasons to study slow light (SL). Clearly, the concept of SL is in direct opposition to our daily life experience of light traveling extremely fast. The fundamental interest is to have a deeper and better understanding of light propagation and light-matter interactions under circumstances where the effective velocity of light is much lower than the usually considered speed, $c = 3 \times 10^8$ km/s. In addition, there is huge technological interest for improvement of optical devices where requirements such as power, low–loss and compactness can be addressed with SL concepts. One of the main issues in the modern communication links is electro–optical conversion where a lot of energy is lost and at the same time the speed of information transfer is decreased. An all optical integrated circuit that can substitute the role of electronics would significantly improve a communication link. For practical implementation SL could actually allow faster optical communication [1, 2, 3]. In such cases, planar photonic crystal (PC) is a very promising platform where various optical functionalities can be integrated on the same device. Figure 1.1 shows an imagined photonic chip where components such as buffers, optical memories, amplifiers and delay lines are crucial parts of such a device. All these devices take advantage of the SL phenomena that has to be understood in detail.

The concept of group velocity v_g describe the propagating speed of the light pulse. SL refers to situations where v_g is much smaller than the light velocity in the vacuum. In simple terms, we can obtain SL in two ways.

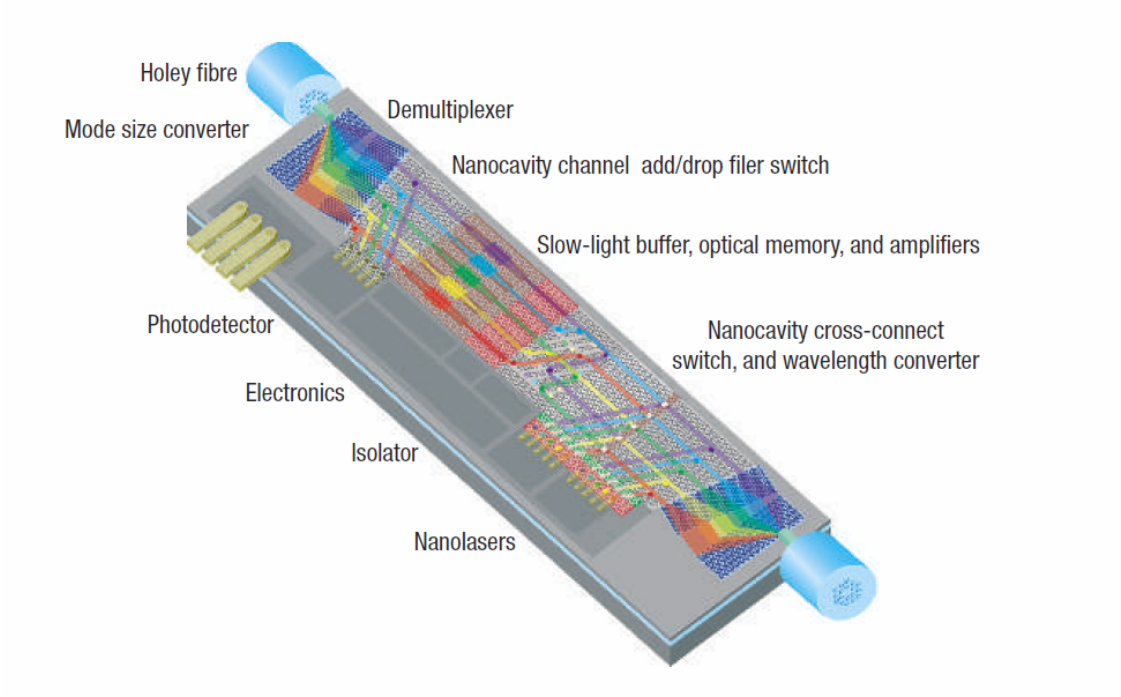

Figure 1.1 The photonic chip, from ref. [4].

First, by changing dispersive properties of homogeneous media with various schemes as: electromagnetically induced transparency (EIT) [5], coherent population oscillation(CPO) [6], stimulated Brillouin scattering(SBS) [7]. Second, by periodically pattering homogeneous dielectric media. In the first case strong dispersion occurs due to atomic resonances while in the second case it is due to geometrical resonances. The famous experiment performed by Hau *et al.* [5] in 1999, belong to the former example. Together with the co–workers she showed that light pulses can be slowed down to a speed of 17 m/s. This experiment was definitely one of the milestones for the research in the SL. But, such experiment requires very complicated and large set–up that is impractical for any real application outside a lab environment. On the other hand, ideal periodic structures can offer very low v_g based on very small sample footprints, which fulfill integration requirements.

Properties of fabricated structures are affected by various structural and material [8, 9] sources of imperfections that jeopardize SL properties. It is necessary to understand physics behind these processes in order to make more

robust and reliable devices. On the other hand, enhancement of light–matter interaction in periodic structures [10, 2, 11] is one of the most appealing features of structural SL. Therefore, in this thesis, we are interested in two central aspects of SL. First, the limitation of the real structures where various sources of imperfections will compromise minimum group velocity v_g is considered. Second, the enhancement of the light–matter interaction due to SL in periodic media is investigated. The limitations of v_g have important implications on enhancement of light–matter interaction. These two effects are tightly related, and therefore, it is necessary to study both effects simultaneously and on equal footing. We show that SL enhancement in periodic media of light–matter interaction is limited by the amount of introduced homogeneous loss/gain.

1.1 Thesis outline

The thesis is structured as follows:

Chapter 2 The necessary theoretical background is presented. First we introduce Maxwell's equations from which the eigenvalue problem for a periodic media. We touch upon the Kramers–Kronig relations for dielectric materials. The chapter is concluded with a discussion on different definitions for pulse speed and the meaning of the superluminal group velocity.

Chapter 3 We briefly discuss material SL in the first section and in much detail SL in periodically structured media. In the first section we go through the most important SL methods in homogeneous material where the speed of light is reduced due to the strong material dispersion. Methods for material SL are explained in the first section. EIT is still very challenging to implement on room temperatures, while CPO seems very promising. SBS and Stimulated Raman scattering (SRS) are both very versatile processes and with wide tunable range which make them very attractive. Three guiding SL structures are of central interest in this thesis. In the following subsections we explain their features with emphasize on SL properties. The coupled resonator optical waveguide (CROW) is very easy to study because the dispersion relation can be calculated in a closed form. Therefore SL

and other physical properties can be easily understood. Then the ideal photonic crystal waveguide (PCW) is introduced, in this case it is necessary to perform numerical calculations in order to calculate the dispersion. In the end, the hollow core fiber (HCF) is introduced. Our fiber has a very big hollow,compared to the standard HCFs, core that support SL light modes.

Chapter 4 Limitations of SL in various structures: CROWs, PCW and briefly also HCFs. This is done by introducing an imaginary part to the dielectric constant. By implementing analytical and numerical methods we are able to predict the same qualitative behavior of the limitations of SL.

Chapter 5 The enhancement of loss and gain has been explored, using existing knowledge from Chapter 4. Even though gain and loss seem fundamentally different they are found to have the same effect on the dispersion. That gives rise to a limitation of the enhancement of light-matter interaction.

Chapter 6 To conclude this thesis we provide a summary and discussion of the main results obtained together with a brief outlook at the future.

2

Electromagnetism in periodic structures

Starting from Maxwell equations, we derive a wave equation for homogeneous and periodic materials. These equations are the essential ingredients for analysis of periodic structures. Using a representation of the electromagnetic problem in an operator form, concepts from solid state physics such as Bloch waves and Bloch wavevectors are used to describe the waveform in the periodic media. For any physical system causality condition has to be satisfied, we show how causality leads to Kramers–Kronig relations. Moreover Kramers–Kronig relates imaginary and real part of the complex dielectric constant, in other words they show how dispersion and absorption of material are related. In the end, we derive group velocity for a propagating pulse that allow us to introduce concepts of slow and fast light.

2.1 Maxwell's equation

Classical electromagnetic phenomena can be explained with a set of four coupled partial differential equations. Any electromagnetical law can be deducted from these equations. The set of Maxwell equations [12] is the

following:

$$\nabla \times \mathbf{E} = -\frac{\partial \mathbf{B}}{\partial t} \tag{2.1}$$

$$\nabla \times \mathbf{H} = \frac{\partial \mathbf{D}}{\partial t} + \mathbf{J} \tag{2.2}$$

$$\nabla \cdot \mathbf{D} = \rho \tag{2.3}$$

$$\nabla \cdot \mathbf{B} = 0 \tag{2.4}$$

The electric field is represented by $\mathbf{E}$ and the magnetic field is $\mathbf{H}$, $\mathbf{B}$ is the magnetic flux density and $\mathbf{D}$ the dielectric displacement, $\rho(\mathbf{r})$ is the charge distribution and the $\mathbf{J}$ the current density. All fields, charge distribution and densities are functions of space and time. The continuity equation:

$$\nabla \cdot \mathbf{J} + \frac{\partial \rho(r)}{\partial t} = 0 \tag{2.5}$$

is implicitly given in the Maxwell equations and it can be obtained from eq. 2.2 and eq. 2.3.

Maxwell equations are very general and can deal with any type of electromagnetic problems. Dielectric permittivity ϵ and magnetic permeability μ contain properties of medium where the electromagnetic field is present. In general these two quantities are tensors in which each tensor element depends on space and time. We will make assumptions about the medium that will help us to describe the electromagnetic problem. It is reasonable to assume that $\mu = 1$,since all media that we will study have magnetic response equal to unity. It is useful for now to make the assumption that the medium is homogeneous, meaning that ϵ does not depend on $\mathbf{r}$. Later on, we will relax this assumption, because we are going to deal with periodic media which are obviously spatially dependent. The medium is isotropic, meaning that dielectric tensor $\bar{\epsilon}$ is

$$\bar{\epsilon} = \begin{bmatrix} \epsilon & 0 & 0 \\ 0 & \epsilon & 0 \\ 0 & 0 & \epsilon \end{bmatrix} \tag{2.6}$$

. This assumption immediately reduces $\bar{\epsilon}$ from being a tensor to scalar. Then

we assume (for now) that the medium is time independent. We will assume that media is linear, ϵ does not depend on poweres of $\mathbf{E}$ [13, 14]. All these assumptions yield very simple constitutive relations for electric and magnetic field. The constitutive relations connect the fields $\mathbf{D}$, $\mathbf{B}$ and $\mathbf{J}$ to the fields $\mathbf{E}$ and $\mathbf{H}$. The field $\mathbf{D}$ is related to the field $\mathbf{E}$ through the dielectric function ϵ where

$$\mathbf{D}(\mathbf{r}) = \epsilon_0 \epsilon \mathbf{E}(\mathbf{r}) \tag{2.7}$$

for the fields $\mathbf{B}$ and $\mathbf{H}$ we have simply

$$\mathbf{B}(\mathbf{r}) = \mu_0 \mathbf{H}(\mathbf{r}) \tag{2.8}$$

while for $\mathbf{J}$ and $\mathbf{E}$ relation is

$$\mathbf{J}(\mathbf{r}) = \sigma \mathbf{E}(\mathbf{r}) \tag{2.9}$$

where σ is electrical conductivity.

In order to get the wave equation, we will disregard sources of electromagnetic field $\rho(\mathbf{r})$, $\mathbf{J}(\mathbf{r})$ and, with previous assumptions about the medium, the Maxwell equations become

$$\nabla \times \mathbf{E} = -\mu_0 \frac{\partial \mathbf{H}}{\partial t} \tag{2.10}$$

$$\nabla \times \mathbf{H} = \epsilon \epsilon_0 \frac{\partial \mathbf{E}}{\partial t} \tag{2.11}$$

$$\nabla \cdot \mathbf{E} = 0 \tag{2.12}$$

$$\nabla \cdot \mathbf{H} = 0 \tag{2.13}$$

Applying the operator $\nabla\times$ to eq. 2.10 and bearing eq. 2.12 in mind that we get the wave equation in vacuum ($\epsilon = 1$)

$$\nabla^2 \mathbf{E} + \frac{1}{c^2} \frac{\partial^2 \mathbf{E}}{\partial t^2} = 0 \tag{2.14}$$

where $c = 3 \times 10^8$ [m/s] is the speed of light and is given by

$$c = \frac{1}{\sqrt{\epsilon_0 \mu_0}} \tag{2.15}$$

We can obtain a wave equation for $\mathbf{H}$ just doing the same operation that we did for eq. 2.10 with but now with eq. 2.11. Assuming harmonic time dependence of $\mathbf{E}(\mathbf{r}, t)$ and $\mathbf{H}(\mathbf{r}, t)$ the wave equations turns into the following form:

$$\nabla^2 \mathbf{E} - \left(\frac{\omega}{c}\right)^2 \mathbf{E} = 0 \tag{2.16}$$

$$\nabla^2 \mathbf{H} - \left(\frac{\omega}{c}\right)^2 \mathbf{H} = 0 \tag{2.17}$$

with superposition of plane waves we can get solution for an arbitrary waveform. The electromagnetic problem from aforementioned equations is solved together with proper boundary conditions.

The periodic medium implies that ϵ is a function of space $\epsilon(\mathbf{r})$. Doing the same mathematical steps that we did previously for the homogeneous case we get the equations that take into account the inhomogeneous nature of the material

$$\nabla \times \nabla \times \mathbf{E} = \epsilon(\mathbf{r}) \left(\frac{\omega}{c}\right)^2 \mathbf{E}, \tag{2.18}$$

$$\nabla \times \frac{1}{\epsilon(\mathbf{r})} \nabla \times \mathbf{H} = \left(\frac{\omega}{c}\right)^2 \mathbf{H}. \tag{2.19}$$

Solving one of these equations we find the waves supported by the periodic medium. We can represent eq. 2.18 and eq. 2.19 as an eigenvalue problem with corresponding operators [15]. The linear operator acting on $\mathbf{H}$ is $\hat{\mathbf{A}} = \nabla \times 1/\epsilon(\mathbf{r}) \nabla \times$ and we can write the eq. 2.19 in compact form as

$$\hat{\mathbf{A}} \mathbf{H} = \left(\frac{\omega}{c}\right)^2 \mathbf{H} \tag{2.20}$$

where $(\omega/c)^2$ is the eigenvalue. The reason why we decided to use equation 2.19 is that linear operator $\hat{\mathbf{A}}$ is hermitian $\left\langle \hat{\mathbf{A}} H_1 | H_2 \right\rangle = \left\langle H_1 | \hat{\mathbf{A}} H_2 \right\rangle$ [16, 15].

A hermitian operator yields important properties for the eigenvalue problem, eigenfunctions corresponding to different eigenvalues are orthogonal, eigenvalues are positive and real. Equation 2.19 is usually called the master equation.

2.2 Bloch wave theory

The Bloch theorem has important consequences in development of semiconductor theory, motion of electrons in periodic potentials [17, 18]. It states that eigenfunctions of the wave equation for periodic potentials are the products of plane waves with wavevector $\mathbf{k}$ times a periodic function that has the periodicity of the crystal lattice [17]. Actually the Bloch theorem is a direct consequences of discrete translational symmetry in a crystal [16, 15]. In our case the periodic potential is the dielectric constant

$$\epsilon(\mathbf{r} + \mathbf{a}) = \epsilon(\mathbf{r}) \tag{2.21}$$

where $\mathbf{a}$ is the lattice constant. The operator $\hat{\mathbf{A}}$ is periodic due to periodicity of $\epsilon(\mathbf{r})$ meaning that the eigenfunction $\mathbf{H_k}$ will be of the following form:

$$\mathbf{H_k}(\mathbf{r}) = e^{i\mathbf{kr}}\mathbf{u_k}(\mathbf{r}) \tag{2.22}$$

where $\mathbf{u_k}(\mathbf{r})$ is the periodic function of period a. The plane wave transmitted through the periodic media is spatially modulated by the function $\mathbf{u_k}(\mathbf{r})$ [15]. The solution $\mathbf{H_k}$, where the periodic function $\mathbf{u_k}(\mathbf{r})$ is multiplied by the plane wave is called the Bloch function. Translational and discrete translational symmetry yields different types of wave functions. In the case of continuous translational symmetry the corresponding wave functions are plane waves, while for the discrete translational case wave functions are Bloch waves. The formulation using Bloch wave theory gives rise to an altered dispersion relation.

2.3 Kramers–Kronig relations

The mathematical relation between absorption and dispersion is known as the Kramers–Kronig relations. The imaginary and real part of the complex refractive index $n = n(\omega)' + in(\omega)'' = \sqrt{\epsilon(\omega)} = \sqrt{\epsilon(\omega)' + i\epsilon(\omega)''}$ depend on each other [12]. If imaginary part $n(\omega)''$is known then the real part $n(\omega)'$ is also completely determined. A very important characteristic of the Kramers–Kronig relation is that media that fulfilled these relations are causal [19, 20]. The causality is of extreme importance since every physical system must be causal. It means that no effect can occur before the excitation or that no output exist before the input. Mathematically causality can be formulated in the following way, $F_{in}(t)$ is the input signal that gives F_{out} as the output and $G(t)$ is a transfer (Green) function of the system. We have

$$F_{out}(t) = \frac{1}{\sqrt{2\pi}} \int_{-\infty}^{\infty} G(\tau) F_{in}(t-\tau) \mathrm{d}\tau \tag{2.23}$$

where $G(\tau) = 0$ for $\tau < 0$. The requirement for causality can be expressed by introducing the Heaviside step function

$$U(t) = \begin{cases} 0 & \text{if } t \leq 0 \\ 1 & \text{if } t > 0 \end{cases} \tag{2.24}$$

and then representing $G(t)$ as

$$G(t) = G(t)U(t) \tag{2.25}$$

Performing the Fourier transform of Eq. 2.25 yields

$$\tilde{G}(\omega) = \mathcal{F}\{G(t)U(t)\} \tag{2.26}$$

where we get the following expression

$$\tilde{G}(\omega) = \frac{i}{\pi} P \int_{-\infty}^{\infty} \frac{\tilde{G}(\omega')}{\omega' - \omega} \mathrm{d}\omega' \tag{2.27}$$

The integral is performed in the complex plane and P stands for principal value. The imaginary and real part of $G(\omega)$ can be separated where interdependence between them becomes more clear

$$\mathrm{Re}\left\{\tilde{G}(\omega)\right\} = \frac{1}{\pi} P \int_{-\infty}^{\infty} \frac{\mathrm{Im}\left\{\tilde{G}(\omega')\right\}}{\omega' - \omega} \mathrm{d}\omega' \tag{2.28}$$

$$\mathrm{Im}\left\{\tilde{G}(\omega)\right\} = -\frac{1}{\pi} P \int_{-\infty}^{\infty} \frac{\mathrm{Re}\left\{\tilde{G}(\omega')\right\}}{\omega' - \omega} \mathrm{d}\omega' \tag{2.29}$$

In the upper half plane the function $G(\omega)$ has to be analytic and has to decay fast as $\omega \to \infty$ in order to satisfy the Kramers–Kronig relation. These relations are nothing else but Hilbert transform between real and imaginary part of the complex function $G(\omega)$.

For dispersive media the $\mathbf{D}$ and $\mathbf{E}$ field are related in the following way

$$\mathbf{D}(\mathbf{r}, t) = \int_{-\infty}^{\infty} \epsilon(t - t') \cdot \mathbf{E}(\mathbf{r}, t') dt' \tag{2.30}$$

where we can see the analogy with eq. 2.23, so $\epsilon(t)$ is the response function for excitation field $\mathbf{E}(\mathbf{r}, t)$. Performing the Fourier transform on 2.30 the convolution becomes simple multiplication in the frequency domain $\mathbf{D}(\mathbf{r}, \omega) = \epsilon(\omega)\mathbf{E}(\mathbf{r}, \omega)$ [12]. Since every physical system has to be causal $\epsilon(\omega)$ satisfies the Kramers–Kronig relations

$$\mathrm{Re}\left\{\epsilon(\omega)\right\} = 1 + \frac{1}{\pi} P \int_{-\infty}^{\infty} \frac{\mathrm{Im}\left\{\epsilon(\omega')\right\}}{\omega' - \omega} \mathrm{d}\omega' \tag{2.31}$$

$$\mathrm{Im}\left\{\epsilon(\omega)\right\} = -\frac{1}{\pi} P \int_{-\infty}^{\infty} \frac{\mathrm{Re}\left\{\epsilon(\omega') - 1\right\}}{\omega' - \omega} \mathrm{d}\omega' \tag{2.32}$$

Complex refractive index $n = \sqrt{\epsilon' + i\epsilon''}$ can be expressed with approximate expression $n \cong \sqrt{\epsilon'} + i\epsilon''/(2\sqrt{\epsilon'})$ in the case when $\epsilon'' \ll \epsilon'$. It is very important to bear in mind that this approximated expression does not formally fulfill the Kramers–Kronig relations, but the physics of slow light can be correctly analyzed for resonant media [21].

As an example, in fig. 2.1 we show the real and imaginary part of $n(\omega)$ for

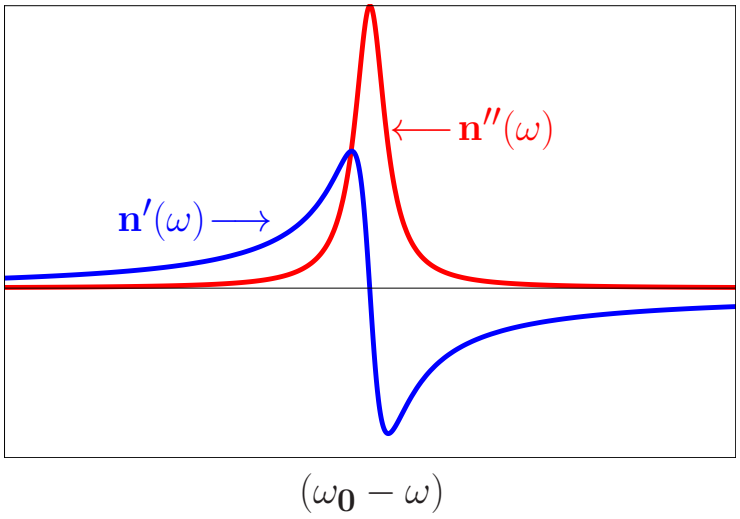

Figure 2.1 Complex refractive index associated with two level system

a two level sytem where we can see that significant absorption occurs only around resonant (red line) frequency ω_0 and in correspondence with a high absorption there is steep change in real part n' (blue line).

2.4 Group velocity

Monochromatic waves propagate in a medium with a phase velocity

$$v_\varphi = \frac{\omega}{k} = \frac{c}{n} \tag{2.33}$$

where n is the refractive index of hosting medium. Waves generated from a highly precise source is not single frequency but it has a small bandwidth $\Delta\omega$ and the k wavevector spectrum is also finite [12]. A light pulse is a superposition of an infinite number of plane waves centered around the wavevector k_0. With Fourier transform we can reconstruct the waveform of the pulse. The dispersion relation shows the dependence between ω and k. In the most general case ω and k are complex quantities, but we will assume that both are real. The propagating pulse $u(z,t)$ is described by the Fourier integral [12],

$$u(z,t) = \frac{1}{\sqrt{2\pi}} \int_{-\infty}^{\infty} A(k) e^{ikz - i\omega(k)t} \mathrm{d}k. \tag{2.34}$$

The amplitude $A(k)$ is a spectrum of $u(z,t)$ at the time $t = 0$ in the transformed space k

$$A(k) = \frac{1}{\sqrt{2\pi}} \int_{-\infty}^{\infty} u(z,0) e^{-ikz} \mathrm{d}k \tag{2.35}$$

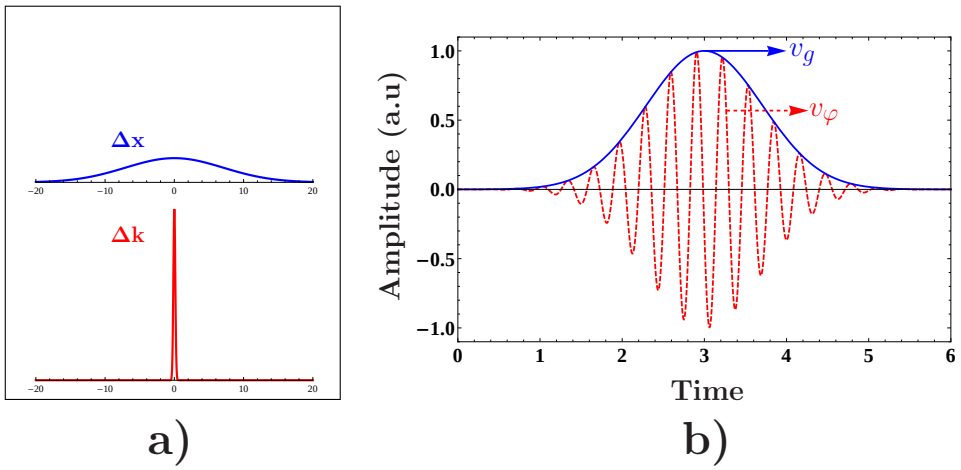

Figure 2.2 a) Very slowly varying pulse shape in the real space and the very peaked pulse when it is transformed to Fourier space. b) Pulse envelope (in blue) propagating with v_g and carrier frequency (red dashed line) propagating with v_φ

Pulses whose power is peaked around k_0 (i.e. Δk is very small) have an amplitude that varies slowly in the space domain. In the panel a) of fig. 2.2 we see how a very broad pulse in the space domain is very peaked in the transformed k space. We Taylor expand $\omega(k)$ around k_0

$$\omega(k) \cong \omega_0 + \frac{d\omega}{dk}(k - k_0) + O(k^2) \tag{2.36}$$

. When we put the 2.36 in Eq. 2.34 we get

$$u(z,t) \cong \frac{e^{i(k_0 \frac{d\omega}{dk} - \omega_0)t}}{\sqrt{2\pi}} \int_{-\infty}^{\infty} A(k) e^{i[kz - \frac{d\omega}{dk}t]} \mathrm{d}k \tag{2.37}$$

the expression under the integral in the Eq. 2.37 is the same as Eq. 2.35, with a new variable $z' = z - (d\omega/dk|_0)t$. We thus basically represent the pulse in the moving frame scheme. As the pulse propagate though the medium it will

maintain its shape and will propagate with speed known as group velocity

$$v_g = \frac{d\omega}{dk}. \tag{2.38}$$

Writing the pulse expression in the more compact form

$$u(z,t) \cong u(z - tv_g, 0)e^{i[k_0 v_g - \omega_0)]t} \tag{2.39}$$

the slowly varying envelope $u(z',0)$ propagates through the medium with velocity v_g while the plane wave propagate with phase velocity, see the illustration on fig. 2.2 b). Neglecting all higher order terms in the expansion eq. 2.36 means that the pulse preserves its shape along the propagation through the medium. From the dispersion $\omega = \omega(k)$ relation we can express the group velocity as

$$v_g = \frac{c}{n + \omega(dn/d\omega)} = \frac{c}{n_g} \tag{2.40}$$

where the quantity n_g is called the group index. In fig. 2.3, n_g spectrum of two level system is illustrated.

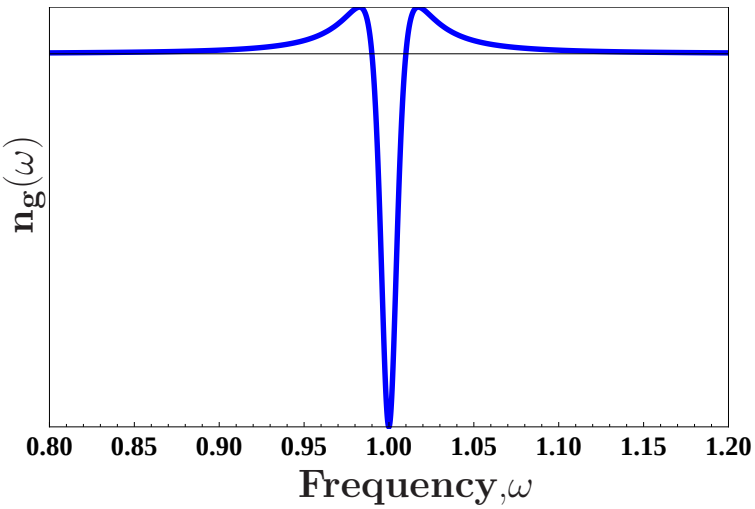

Figure 2.3 Group index spectrum for two level system

Depending on $dn/d\omega$ we have *anomalous*, *normal* dispersion regions and dispersionless region. In the anomalous dispersion region, the quantity $dn/d\omega < 0$ means that light is propagating with fast or superluminal velocity, while

for a $dn/d\omega > 0$ we are in the regime of the slow light; and in the dispersionless region the quantity is $dn/d\omega \cong 0$. The superluminal pulse propagates with speeds higher than c. This seems to be in contradiction with special relativity, which states that nothing can propagate faster than the velocity of light in vacuum. In the following section we will touch upon the concept of fast light and see how it can be understood and interpreted. Slow light (SL) has a central role in this thesis and following chapters will focus on different aspects of SL in periodic structures and the effect on the light-matter interaction.

In the derivation of the group velocity we neglected high–order derivatives in the expansion eq. 2.36 meaning that no dispersion will influence the pulse shape along the propagation. For very short pulses with a time width T_0, higher order coefficients $\beta_2 = d^2k/d\omega^2$ and $\beta_3 = d^3k/d\omega^3$ from eq. 2.36 have to be taken into account. The group velocity dispersion (GVD) is represented by β_2 and it quantifies how much a pulse is going to spread. The coefficient β_3 is third order dispersion that acts asymmetrically on the pulse shape [14]. The effect of two higher order dispersions becomes relevant when the dispersion length

$$L_D = \frac{T_0^n}{\beta_n}, n = 2, 3 \tag{2.41}$$

is smaller or comparable with the propagation distance [14]. For very short pulses and very long propagation distances, these effects will significantly modify the pulse shape, where v_g as a quantity that defines pulse propagation lose it physical meaning. A light pulse tends to spread and distort as it propagates through a material. For this reason, it is not possible to use a single definition of velocity to describe the speed at which a pulse of light propagates through the material [22, 20]. The following definitions are used to describe properly the pulse speed:

- Front velocity: the propagation velocity of the front of a step-function discontinuity

- Signal velocity: is defined operationally as the velocity of propagation of the half-the-peak-intensity point on the leading part of the pulse.

- Energy velocity: This is approximately equal to the group velocities when the frequency of the field is far from any absorption (or amplification) resonances but near resonances theoretically it can appear to be superluminal if we do not take proper account of the fact that energy is stored for a finite time in the medium.

When interferences are such that the pulse peak appears to travel with v_g higher than c we are in the superluminal regime. But Einstein's special theory of relativity says that: no signal can propagate faster than the speed of light in a vacuum. As we mentioned before, the v_g doesn't always have physical meanings, because of strong dispersion and absorption that can drastically change the pulse profile leading to erroneous interpretation of pulse speed. Points of discontinuity propagate at the speed of light in a vacuum because no physical material can respond instantaneously to a change in a waveform [23]. Superluminal speed of light is just an artifact of our definition of v_g. The signal velocity is always subliminal, even when the apparent group velocity is superluminal [24]. So, causality is always satisfied.

As an example, n_g can be manipulated in two ways in order to get fast light, one is using dispersive contribution from $dn/d\omega < 0$ that yields anomalous dispersion and another is to design artificial materials (metamaterials) that have high negative refractive index. In metamaterials [25] negative n_g implies that the peak of the pulse travels in a direction opposite to that of its phase velocity and to that of energy flow [26]. Some exotic propagation effects can occur when light pulses pass through a dispersive material, as we can see from fig 2.4. One of these is superluminal pulse propagation. In (A), a 260-ns-long (full width at half maximum) pulse propagates through a laser pumped potassium vapor with n_g of approximately 20 (dashed line). The peak of the pulse is seen to be advanced by 27 ns with respect to vacuum propagation (solid line) [27]. Such superluminal propagation effects may appear to violate principles of causality, but in fact they do not for reasons illustrated in (B). Any real pulse has a "front": the first moment in time at which the intensity becomes nonzero, as indicated by the vertical line. In superluminal propagation experiments, the peak of the pulse moves at a superluminal velocity, but the front of the pulse moves at velocity c. Be-

cause the information is contained in the front of the pulse, no information is transmitted at a velocity exceeding c. For propagation distances longer than those shown here, for which the pulse peak begins to overtake the pulse front, severe pulse distortion always occurs and no pulse energy ever precedes the pulse front. (C) Another exotic propagation effect is backward pulse propagation. This effect occurs for a sufficiently long material with a negative n_g and leads to the result that the peak of the transmitted pulse appears to emerge from the material medium before the peak of the incident pulse enters the medium. Backward propagation has been observed in the laboratory [28]. The plots are based on a simple model that assumes that all spectral components of the pulse propagate without loss at the same v_g [22].

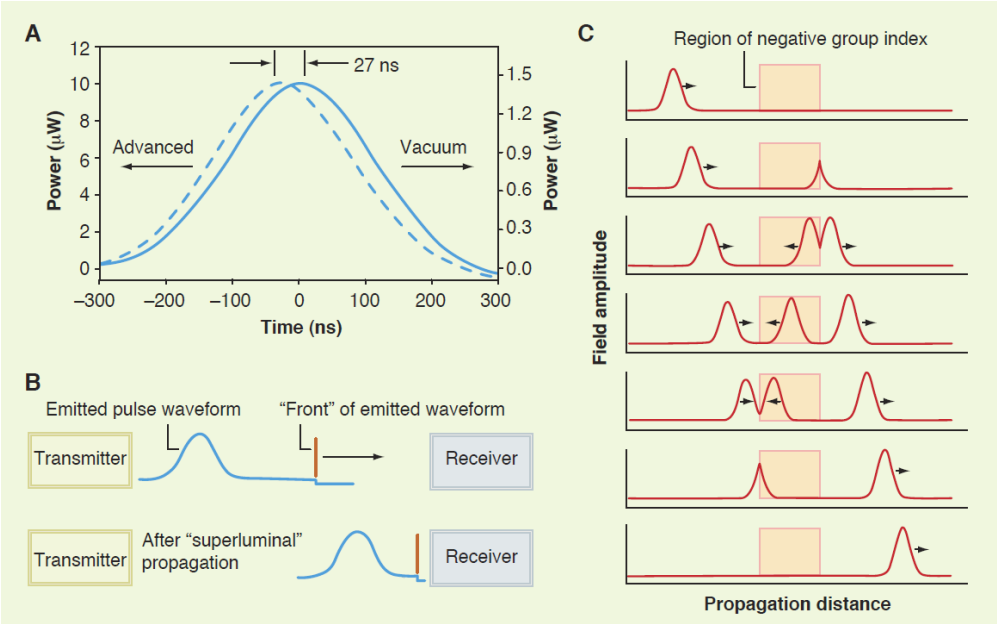

Figure 2.4 A) Superluminal pulse advancement, B) Front of emitted pulse propagation, C) Pulse propagation through the negative index material. Figure from ref [22].

3

Engineering the Speed of Light

The methods for slowing down light are divided into two groups; those based on structural dispersion and others on material dispersion. Here by material dispersion we refer to methods that somehow can change the atomic response of the medium in such a way that a strong dispersion is accompanied with acceptable (or no) loss. In the first section, I will give a brief overview of the most promising methods for material dispersion slow light (SL). The central theme of this thesis are aspects of SL in structured media. Therefore, the following three sections of this chapter are dedicated to the origin of SL in a structured periodic material. Three important structures are explored: coupled resonator optical waveguide (CROW), photonic crystals waveguide (PCW) and photonic crystal fibers (PCF).

3.1 Material Dispersion

Electromagnetically induced transparency (EIT) is a quantum mechanical phenomenon based on destructive quantum interference. The optical response of the medium is modified by a strong pump field that introduces change in the optical pathways of absorption for the probe field. The effect relies on maintaining the quantum coherence between states [29]. By doing this, absorption at the resonant frequency is almost completely eliminated while dispersion is completely changed [30]. In other words a medium that was opaque at resonant frequency ω_0 with anomalous dispersion becomes transparent with normal dispersion. A steep dispersion curve and suppressed

absorption imply that SL is possible. The transmission window around ω_0 is very narrow [31] meaning that very broad pulses (in frequency domain) would be severely distorted. While linear absorption is suppressed by the EIT, nonlinear susceptibility is enhanced by constructive interference [30].

In EIT experiment a cloud of extremely cold atoms called a Bose–Einstein condensate (BEC) is used in order to control precisely the energy levels for EIT. Such low temperatures imply that energy states are sharply defined and thereby the frequency range where cancellation occurs can be made very narrow [32].

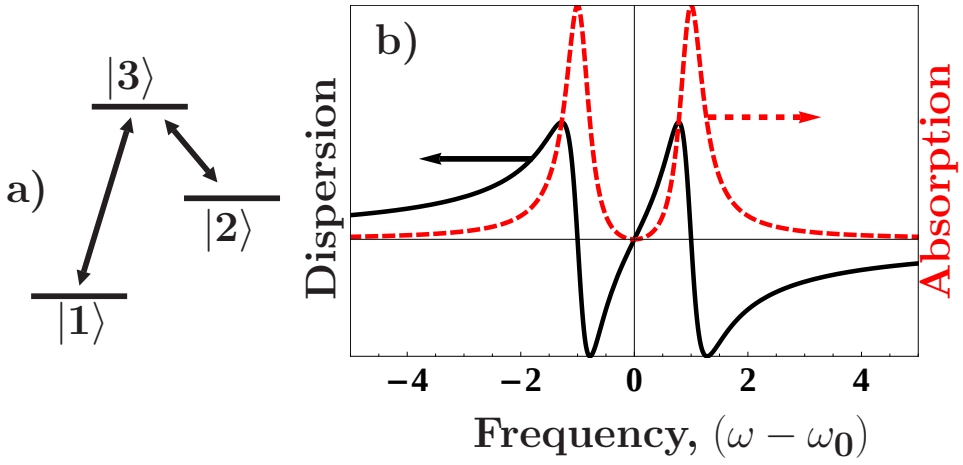

Figure 3.1 a) Three–level system and b) Absorption and dispersion associated with EIT.

From panel a) in the fig. 3.1 we can see a three–level system for EIT. The scheme used is called a "lambda" and it is the most used scheme. There are two other configurations called "ladder" and "vee", but for practical reasons the lambda is preferable [30]. In panel b) we see the absorption spectrum of the BEC with resonant frequency ω_0 after applying the pump field. We can see that two absorption peaks are equally separated from ω_0 and that absorption around ω_0 is completely suppressed. The distance between two absorption peaks depends on the intensity of the pump field, that is denoted as Rabi frequency $\Omega_p = \mu E/\hbar$ where μ is the dipole moment, E is the electrical field amplitude and $\hbar$ is the Planck constant. The panel b) shows an anomalous dispersion region around resonant frequency ω_0 but when the pump is applied, the dispersion changes drastically. The refractive index of

EIT medium at ω_0 is almost 1 [31]. Dispersion becomes normal and very steep around ω_0 meaning that v_g will be very low. What is more interesting, by changing the Ω_p we can change v_g. But we should be careful about the trade–off: if Ω_p is decreased, the dispersion curve will be steeper, but at the same time two absorption peaks will get closer and that will increase absorption around ω_0.

Performing experiments at cryogenic temperatures is very interesting and a variety of exciting phenomena can be studied, but is unsuitable for any on–chip applications. One of the possible solutions for solid state EIT is by introducing quantum dots (QD) on semiconductor substrates [33, 34]. The problem with QDs is that they suffer form high dephasing rates compared to BEC and inhomogeneous broadening due to the fluctuation in size [35]. It is very challenging to reach very long dephasing times in semiconductors even at low temperatures due to interaction with phonons of the crystal lattice [34]. One possibility is to combine a photonic crystal waveguide together with QDs. In that way it is possible to control and enhance n_g by using SL effects due to EIT and PC waveguide dispersion [36]. Implementation of EIT on chip has recently been demonstrated [37]. Filling a hollow core planar waveguide with hot rubidium vapors, n_g of 1200 with transparency of 0.44 has been obtained [37]. This is a very significant and encouraging result that puts really good prospectives for EIT for on–chip applications.

Another possibility to obtain slow light at room temperature is coherent population oscillation (CPO). The material is excited with the modulated wave meaning that we beat continuous wave (CW) of frequency ω_0 with a wave of slightly lower frequency. The high intensity wave creates a frequency region $\Delta\omega$ where absorption/gain becomes depleted [21]. Having a dip in the absorption spectrum means that the refractive index will change due to Kramers–Kronig relations. High values of n_g [6] are obtained, meaning that significant slowdown of the probe pulse occurs, see the illustration in fig. 3.2.

From panel a) fig. 3.2, we can see that the pumping frequency is interacting with a continuum of states. The carrier density is modulated by the strong pump field, resulting in a dip in the absorption spectrum, as shown in panel b). Since the real and imaginary part of the material dispersion are

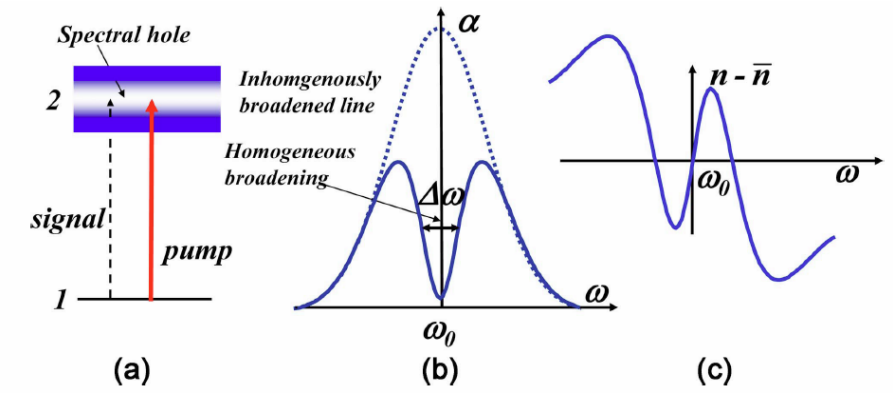

Figure 3.2 a) Two level scheme and b) Absorption and c) dispersion associated with CPO, figure taken from ref. [21].

related by the Kramers–Kronig relation, the dip in the absorption spectrum results in a very abrupt change in refractive index [38], as we can see from panel c).

There are several advantages of CPO with respect to EIT: it does not require coherence between states, it is much less affected by inhomogeneous broadening than EIT. It also has much larger bandwidth than EIT, this is extremely important for high speed applications, and is quite easy to implement in actual semiconductor materials [38, 34]. With all this CPO will probably be the way to go for the future integrated devices where material slow light is required [22].

Processes like stimulated Brillouin scattering (SBS) and stimulated Raman scattering (SRS) are the most promising candidates for a room temperature SL applications in optical fiber technologies. SBS has higher efficiency, it can work with very low pump powers and for almost any wavelength [7]. In SBS, the energy from pump waves modulates the material density creating a time grating (acoustic wave) in the fiber seen from the probe pulse. When matching conditions between pump, probe and generated acoustic waves are fulfilled, energy is transferred from pump to probe [21]. Very narrow gain resonance of SBS means a very steep dispersion curve, implying that the pulse can be significantly slowed [22, 7]. Dispersion is also controlled by power, meaning that n_g can be tuned. The main disadvantage of SBS is that the Brillouin resonance bandwidth is very narrow hence data transmission rates

are quite limited [22]. Another nonlinear process that arises from molecular vibration is SRS. This process has broad bandwidth due to the structural disorder in amorphous materials, but much smaller gain compared to the SBS [21].

3.2 Structural dispersion

3.2.1 Coupled optical resonator waveguides

By arranging in line identical optical resonators we can make a new type of a waveguide called coupled resonator optical waveguide (CROW). Such a waveguide was initially proposed by Yariv *et al.* in 1999 [39]. Wave guiding in CROW is different from total internal reflection (TIR) or Bragg reflection. In the CROW, photons are hopping from one resonator to another by evanescent field coupling. The CROW has been made with different types of resonators: photonic crystal (PC) cavities [40, 41, 42], microspheres [43], microring resonators [44, 45, 46] and Fabry–Perot resonators [47]. Among these different design possibilities, the microring resonators are the more widely used building blocks for CROW. The realization of a microring is simple and a single fabrication step is all that is required; there is no need for ultra-high resolution lithography [48]. Among fabricated structures, only PC CROWs come close compared to microring one, but so far microring CROWs has shown superior quality in terms of flexibility, tunability and, most important, reproducibility [44]. In Figure 3.3 we can see the state of the art of the microring CROW structure.

From resonator properties and established distance between neighboring resonators all waveguide properties are defined. Design flexibility and extremely easy analytical calculation of dispersion relation make them very appealing structures for implementing integrated photonic devices. We will focus on the SL properties of that permit construction of delay lines [49, 50], buffers [45], as well as various nonlinear signal processing [42, 44] and filtering [44]. In fig. 3.4, we can see one example of the CROW waveguide together with parameters that define its dispersive and guiding properties.

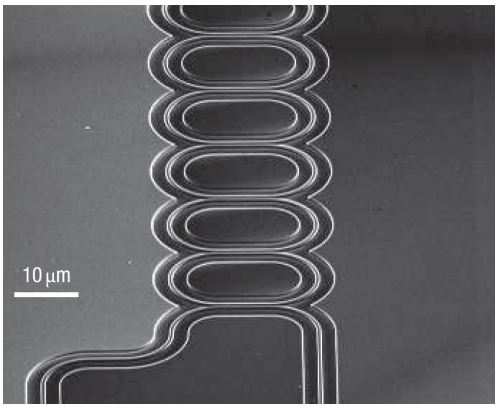

Figure 3.3 State–of–the–art CROW realized on silicon-on-insulator, taken from ref. [45].

The resonant frequency Ω of the single resonator depends on the geometry

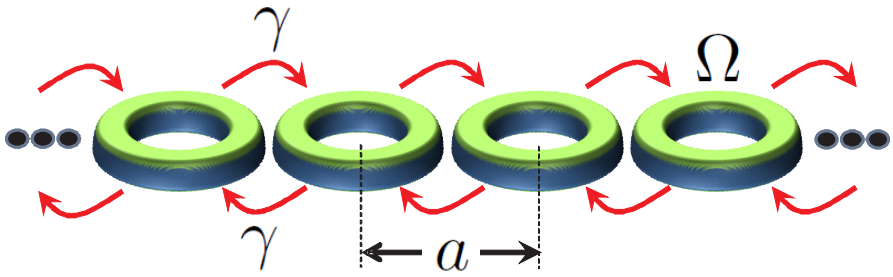

Figure 3.4 CROW waveguide

and material properties of the resonator. Since Ω is the eigenvalue for a given electromagnetical problem, the eigenmode $\mathbf{E}_\Omega(\mathbf{r}, t)$ is the associated electric field distribution. Assuming that the CROW is a chain of an infinite number of resonators we can apply the Bloch theorem, meaning that the electric field can be represented in the following form

$$\mathbf{E}(\mathbf{r}, t) = E_0 \exp(i\omega t) \sum_n \exp(-inka)\mathbf{E}_\Omega(\mathbf{r} - na). \tag{3.1}$$

We will assume that the electromagnetic field is strongly confined in the resonator and that the distance between resonators a, is large enough that coupling occurs only between nearest neighbors. Fields are coupled via evanescent tails that overlap [39], implying weak coupling. The large separation between resonators means that the field distribution of one resonator does

not affect the field of the neighboring one. The only difference from resonator to resonator is the associated phase constant while the field remains the same. The coupling coefficient γ is expressed in the following way

$$\gamma = \int \Delta\epsilon E_\Omega(\mathbf{r}) E_\Omega(\mathbf{r}+a)\mathrm{d}\mathbf{r}. \tag{3.2}$$

The assumption of weak coupling occurs very often in the calculation of band structures in solid state physics [17, 18] where the atomic potential is a function that decays very fast with distance from the center and in that case the method is called tight-binding. Another method that is also widely used for analysis of CROW is transfer matrices [51], in some cases it is convenient to work with coupled mode theory (CMT) in the time domain [49]. If we want to realize CROWs with PC it is possible to calculate the dispersion with the MPB software based on plane wave expansion [52]. Substituting eq. 3.1 in the master eq. 2.18 together with the assumption of weak coupling, we get the dispersion relation

$$\omega = \Omega\left(1 - \frac{\gamma}{2}\cos(ka)\right). \tag{3.3}$$

For the sake of simplicity, we have omitted the term $\Delta\alpha$ in eq. 3.3 that introduces small shifts in the central frequency Ω due to influence of the surrounding (neighboring resonators) [42]. In fig. 3.5 the dispersion curve is shown. Due to the symmetrical properties of the structure, the dispersion is shown just for the positive values of k in the first Brillouin zone. The frequency in the plot has been normalized with the eigenvalue frequency Ω and the wavevector is normalized with a. The derivative of the dispersion relation $\omega(k)$ with respect to k, yields the group velocity

$$v_g = \frac{\partial\omega}{\partial k} = \frac{\Omega a\gamma}{2}\sin(ka). \tag{3.4}$$

What we can see from eq. 3.4, is that at the symmetry point of the Brillouin zone, a light pulse can be stopped formally. In the following chapters we will come back to this issue and analyze this effect on the pulse speed using a more

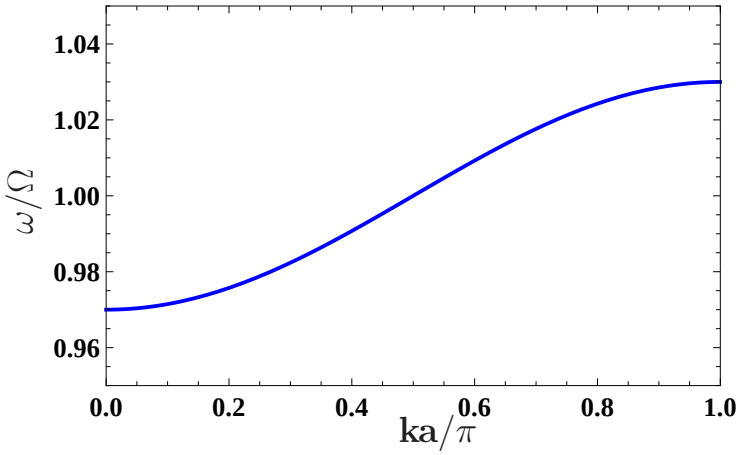

Figure 3.5 Dispersion relation

realistic description. It is clear that the coupling coefficient γ determines max v_g because the steepness of ω depends on γ [48]. Physically, a small γ implies that the photon dwell time in a single resonator will increase and tunneling from site to site will occur with a lower rate. If we would like to decrease the overall v_g in a CROW, we should use a smaller coupling coefficient. But small γ comes with a trade–off with the bandwidth $\Delta\omega$ offered by the structure. In a CROW $\Delta\omega = \Omega\gamma$, meaning that the field confinement and the distance between resonators define the bandwidth, since these two parameters influence field overlap. Having a bigger γ will increase the bandwidth, but the overall v_g would be higher. In panel a) of fig. 3.6, v_g is shown while in b) the GVD is shown.

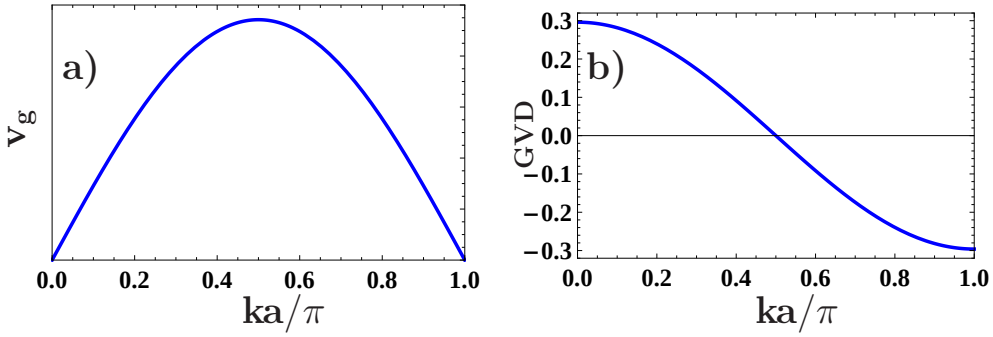

Figure 3.6 a) Group velocity and b) GVD.

From panel b) we can see that the GVD is zero for $ka/\pi = 0.5$; that

corresponds to the single resonator frequency Ω. Close to the band edge, we can reach a very high n_g, but the GVD will be quite strong meaning that the pulse will broaden significantly. If the pulse is centered around Ω then no spreading will occur, but this is also the point with the highest v_g.

3.2.2 Photonic crystals waveguides

Periodical patterning of dielectric media gives new possibilities to control light. Because of a strong similarity to a crystal lattice in solid materials, periodic dielectric materials are called PC. Many new phenomena have been explored in the past years in PC, to name a few: superprism effect [15, 10], slow light [3, 2], and enhancement of light-matter interaction in the linear and nonlinear regime [53, 11, 54]. Photonic crystals were discovered by two scientist at about the same time, Sajeev John [55] and Eli Yablonovitch [56]. Discrete translational symmetry is responsible for strong dispersive properties of PCs that cannot occur in natural materials. Due to the strong index contrast, the wave propagating through the PC is bouncing back and forth hence coupling between forward and backward waves occurs. The waveform that propagates through the PC is a Bloch wave and it has an associated Bloch wavevector k. No propagation modes exist for frequencies in the band gap (BG). In the BG, forward and backward waves interfere in such a way that only evanescent tails exist. In fig. 3.7 we can see fabricated PC structures in 1D, 2D, and 3D

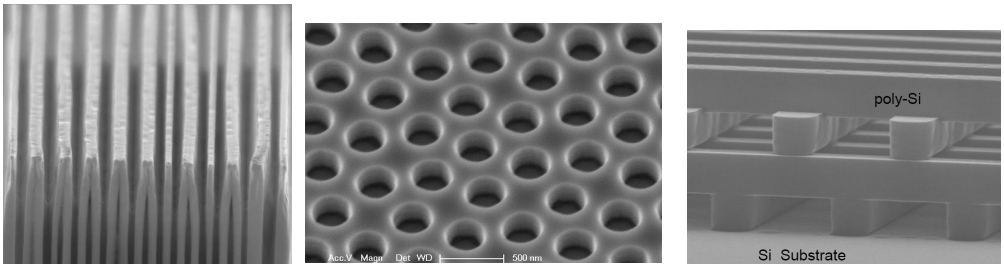

Figure 3.7 a) 1D PC , from [57]. b) 2D PC, from [58]. and c) 3D PC, from [59].

Optical components such as a cavity or waveguide are easily realized in

PCs. For cavities, we need to make a point defect within a structure, while for a waveguide it is necessary to realize a line defect. By introducing defects in the PC we are pulling a mode frequency inside the BG, by doing that light is prevented from propagating in the structure but it is localized or guided (depending on the type of defect)[16, 15]. In traditional waveguides confinement and guiding of light occur due to total internal reflection (TIR) while in PC waveguides (PCW) it is a BG effect that is responsible for guiding and confinement. In the panel a) of the fig. 3.8 we can see an example of a fabricated planar PCW, usually called W1 due to the fact that one line of holes in the PC has been omitted in order to realize the waveguide. While in the panel b) we have the dispersion relation for a W1 waveguide. The normalized frequency is $\omega a/2\pi c$ and normalized wavevector is $ka/2\pi$.

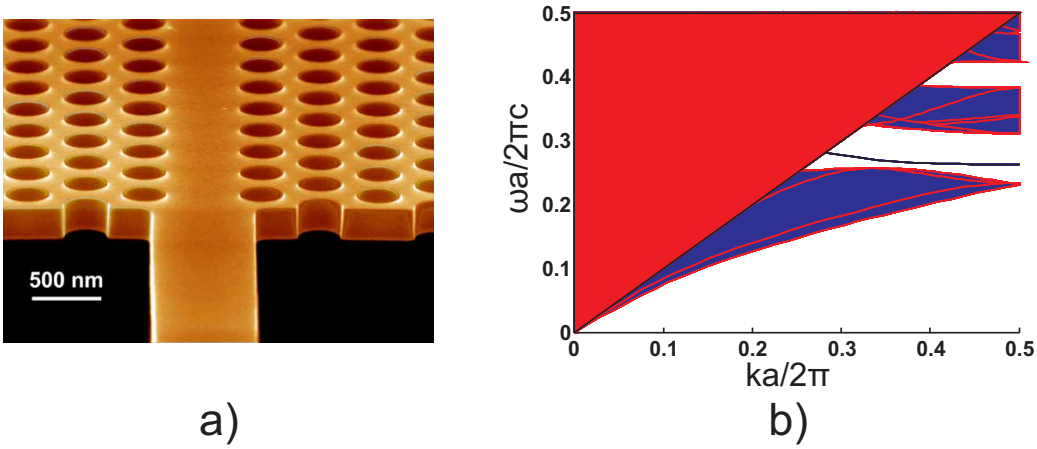

Figure 3.8 a) Fabricated W1 waveguide, from. [60], b) Dispersion curve for W1.

Recently significant progress in fabrication techniques for 3D PCs has been made, although it is still quite difficult to make 3D structures with line or point defects. In order to confine and guide light in 3D we use PC membranes such as the one show in the panel a) of the Fig. 3.8 where light is confined by Bragg reflection in the horizontal plane and in vertical plane confinement occurs due to TIR. Because of the vertical confinement, not all k values are allowed. The red region that covers the upper half of the plot in the panel b) of Fig. 3.8 is called the light cone. All points (ω, k) lying in that area indicate radiative modes [15]. The radiative leakage of energy

occurs due to the fact that the TIR condition is not satisfied and a portion of the wave is transmitted out of the structure.

The particular dispersion that occurs in PCW is mainly due to the periodicity in the horizontal plane. It is a strong scattering of the wave which is bouncing back and forth that is responsible for slowing of light. We can see that the dispersion curve is getting quite flat as we are approaching the symmetry point. The region where the dispersion curve is very flat is called the SL region. In the ideal PC, light can be completely stopped at the symmetry point $ka/2\pi = 0.5$. In real structures, there are various sources of imperfection that are serious obstacles for achieving high values of n_g [9]. Slow light region is accompanied with higher order dispersions [61] that can be a big hindrance for many applications [3, 2]. With a topology optimization method, very robust designs can be made with constant n_g and higher order dispersion can be eliminated [62, 63].

For a 1D structure it is possible to calculate analytically [64] the dispersion. But for 2D and 3D structures, numerical calculations are necessary, if we deal with ideal lossless structures then dispersion can be calculated very efficiently with the MIT free software MPB that implements a plane wave method (PWM) [52]. Various other numerical methods can also be used for more realistic and advanced analysis; a good overview can be found in [65].

3.2.3 Photonic Crystal Fibers

The importance of the optical fiber in the modern communication links is crucial. Low losses (0.18 dB/km), low nonlinearities and good dispersion properties are main requirements for a reliable telecom fiber. For such applications, the most commonly used fiber is a step index fiber, in which guiding is in the most general case based on TIR. In photonic crystal fibers (PCF), guiding occurs due to BG effect or due to the TIR. Due to the very complex geometry and demanding fabricational processes, losses in PCF is still a big issue. But PCF are appealing for applications such as supercountinuum generation, nonlinear application, sensing, dispersion control and amplifier stages where they have superior properties compared to traditional fibers [66, 67]. Three different types of the PCF are shown in the fig. 3.9. In

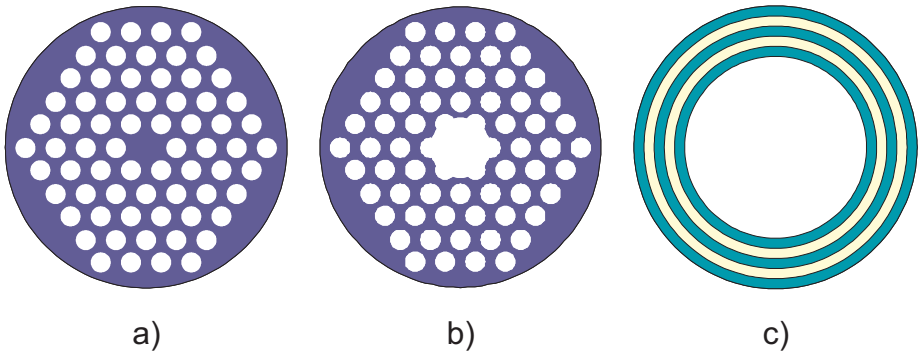

Figure 3.9 a) Solid core PCF, b) Hollow core PCF and c) Bragg fibre.

the panel a) we can see the solid core PCF where guiding is usually based on TIR and the cladding is considered as an effective media. In the hollow core fiber (HCF), panel b), waveguiding occurs due to the band gap effect. The Bragg fiber, panel c), in some sense resembles the circular waveguide used in microwave technology. But here the reflection occurs due to the periodicity of the waveguide walls because use of the metal for reflecting walls would cause unacceptable propagation losses at optical frequencies.

In fig. 3.10 we have an illustration of TIR guiding and guiding in the HCF. In the panel a) we can see how light rays are bouncing against the interface of the dielectric slab and air. Due to TIR, light does not leave the structure but propagates by bouncing against the interfaces. The panel b) shows the electric field distribution in the fiber. We see that light is chiefly confined in the material with high refractive index (inside slab). In the panel c) we can observe how the contribution of the rays reflected from different interfaces confine and guide light in the center hole. Due to the multiple reflections, we can see from panel d) that the electric field is tightly confined in the low index material. Comparing panel b) and d) we can see qualitatively that confinement in the HCF is stronger than in the traditional fiber.

We know from the previous section that creation of defects in perfectly periodic structures leads to localization of light. That is exactly the principle of light confinement in the transversal plane of a PCF. In the projected band diagram for PCF we plot the normalized frequency $\omega a/2\pi$ against $\beta a/2\pi$ that is the normalized wavevector component along the fiber axes. In both cases

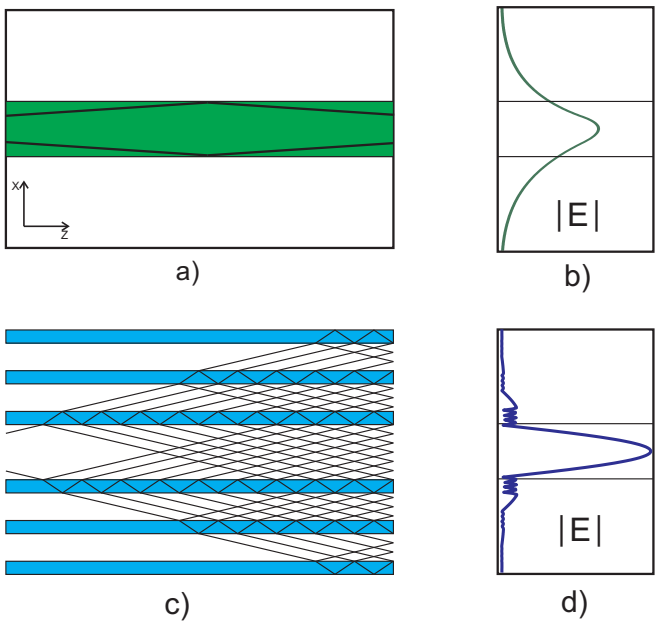

Figure 3.10 a) Light guiding in the fiber, b) Electric field distribution in the fiber, c) Light propagation HCF and d) Electric field distribution in the HCF

normalizations is done with respect to the lattice constant a of the periodic pattern in the transversal plane. The band gap for HCF opens for very big values of β due to the fact that the materials used to make the fibers offer small index contrast [68]. Using glass materials from the family of chalcogenides for fibers it is possible to attain higher index contrasts. If the index contrast is high enough to support a complete BG for all polarizations in the transversal plane, however, then the resulting HCF has a BG extending from $\beta = 0$ to some nonzero β [68]. In the hexagonal lattice we have introduced an air hole of radius $R = 3.38a$. In the Figure 3.11 we can see the BG that opens from $\beta = 0$ and the blue line within BG that is a guided mode in the core. We can see how the dispersion curve of the guided mode is getting flat as it is approaching $\beta = 0$. There is a clear indication that for small values of β, group velocity becomes very low. In the panel c) of Fig. 3.10 it is shown how light waves are bouncing back and forth as they are propagating through the fiber. Small values of β means that light is hitting the interface almost orthogonally. Due to that reason, effective optical path in z becomes much longer. But what is very important is that the majority of the energy

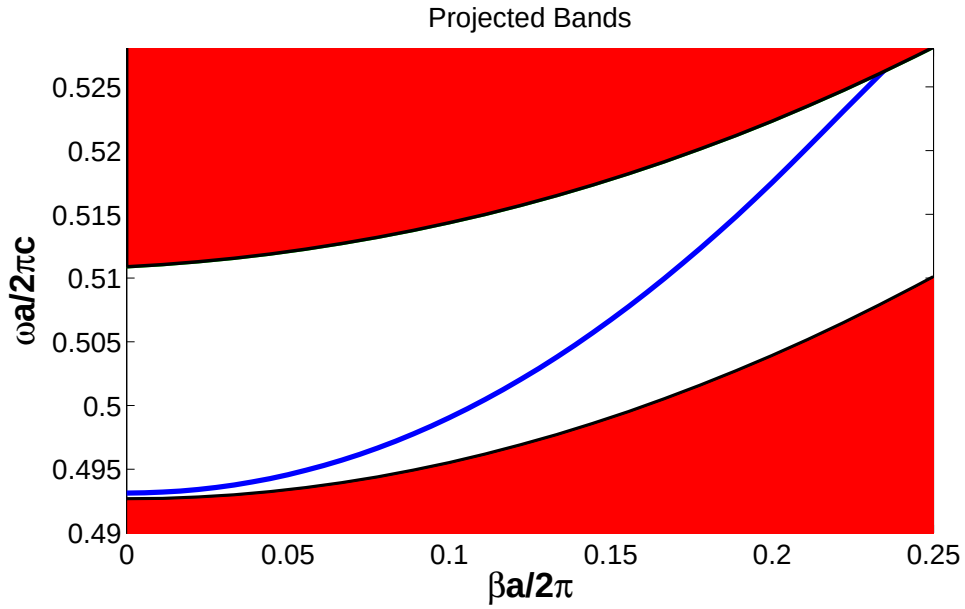

Figure 3.11 Dispersion for hollow core fiber

is still confined within the hollow core. At the same time, we have also strong confinement of the energy inside the core and SL propagation. For various linear and nonlinear processes, this can be a very beneficial situation that can enhance those interactions. But at the same time back action of losses, gain and imperfection will affect SL and in the next chapter we will explore those effects.

4

Limitations of Slow Light in photonic structures

In this chapter I show results from Papers A, B, C, and D where limitations of SL effects are analyzed. The idea is to investigate limitations of n_g in different types of periodic structures where SL occurs. Results for PCW show that the maximum n_g depends on the amount of overall loss mechanisms present in the structure. For CROW, it is possible to study the problem of material losses in a closed form. By adding structural disorder in the CROW together with a finite Q we get further insight into the limitations of SL for such structures. Translationally invariant structures such as HCF are studied with full numerical calculations where we could find the same trend for n_g as in the previous two cases.

4.1 Group index, density of states and limitations in PCW

Planar PCWs are one of the most promising structures for SL applications. It has been demonstrated that very favorable scaling of various phenomena occurs with increase of n_g [3, 2, 69] . In other words, enhancement of absorption/gain [11, 54, 64, 70], nonlinear effects can be enhanced [71, 72, 73] and phase sensitivity is increased [74] by SL effect. Since all these processes depend on n_g we would like to maximize n_g. The fabrication of PC has improved a lot in past years, but the state–of–the–art structures still suffer from structural and material imperfections. These imperfections are sources of

various leakage mechanisms in PCWs such as, radiation losses due to surface roughness, finite size effects [75, 76], intrinsic material losses and scattering losses due to variation in hole radius and position [77, 78, 8]. Electromagnetic energy is lost in the waveguide due to structural and material imperfection. Along the waveguide, the light intensity will be attenuated. Energy leakage mechanisms also affect dispersion and in the proximity of the band edge the effect on dispersion curve is very pronounced. Here we use a semi–analytical approach in order to address the problem of energy leakage. The effect of imperfections is taken into account by introducing a small imaginary part in the dielectric constant. The small imaginary part has a strong effect on SL and that is a reason why n_g values are not higher than ~ 300 [79, 80].

Density of states (DOS) ρ_0 is one of the concepts borrowed from the solid state physics. It gives number of available photonic states (electromagnetic modes) per frequency. For a given electromagnetical problem, e.g. eq. 2.18, we can define the Green's tensor $\hat{\mathrm{G}}$ [76, 81] that allows us to define DOS as

$$\rho(\omega) = \int_V \mathrm{Im}\{\omega \mathrm{Tr}(\hat{\mathrm{G}}(\mathbf{r}, \mathbf{r}, \omega))\} \mathrm{d}\mathbf{r}. \tag{4.1}$$

The volume is indicated with V, while Tr is a trace of the tensor $\hat{\mathrm{G}}$. Then from the $\hat{\mathrm{G}}$ given for a PC [76, 82] we can reformulate the previous equations as

$$\rho(\omega) = \frac{1}{V_{BZ}} \sum_m \int_{BZ} \frac{2}{\pi} \mathrm{Im} \left\{ \frac{\omega}{\omega^2 - \omega_m^2(\mathbf{k}) - i\gamma^2} \right\} \mathrm{d}\mathbf{k}, \tag{4.2}$$

where V_{BZ} is the normalization given by the volume of the first Brillouin zone [82, 83]. Equation 4.2 is a general form of DOS of a periodic structure, where the sum over m indicates different bands and γ is a damping rate that takes losses into account. For an ideal PCW γ is infinitesimal and we are interested in the DOS for a single guided mode that gives

$$\rho_0(\omega) = \frac{a}{\pi} \int \delta\left[\omega - \omega(\mathbf{k})\right] \mathrm{d}\mathbf{k}. \tag{4.3}$$

by the changing integration variable we get

$$\begin{aligned}\rho_0(\omega) =& \frac{a}{\pi}\int \delta[\omega-\omega(\mathbf{k}')]\mathrm{d}\mathbf{k}' \\ =& \frac{a}{\pi}\int \delta[\omega-\omega(\mathbf{k}')]\frac{\mathrm{d}\mathbf{k}'}{\mathrm{d}\omega}\mathrm{d}\omega \\ =& \frac{a}{\pi c}n_g(\omega). \end{aligned} \tag{4.4}$$

We would like to point out that the DOS here is the projected one dimensional DOS in the direction of propagation [84]. From eq. 4.4 it is clear that DOS and n_g are proportional. When we talk about broadening of the electromagnetic modes [83], it is more natural to use DOS, while when we are looking into the slowing down of light we refer to n_g. In the left panel of

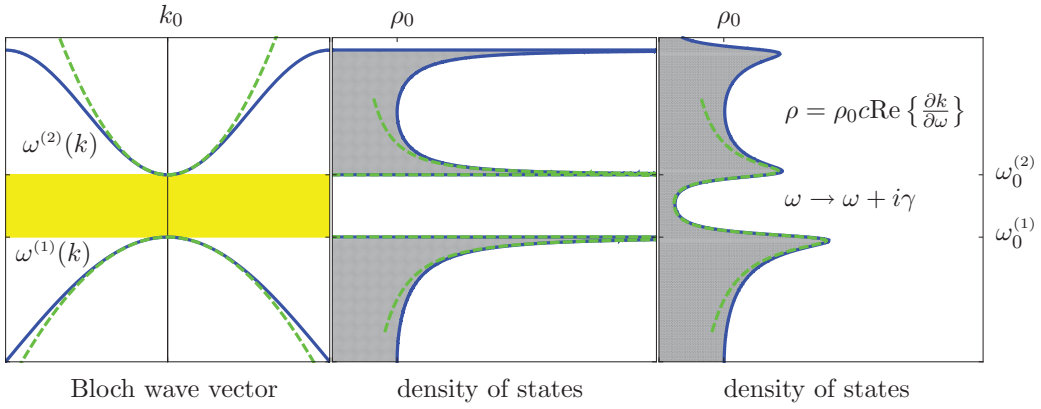

Figure 4.1 Schematic photonic-band structure (solid lines) and the derived photonic density of states. The left panel illustrates the dispersion relation with the parabolic approximation indicated by dashed lines. The middle and right panels show the corresponding density of states for the ideal structure and in the presence of a broadening mechanism, respectively. Figure taken from paper A.

Fig. 4.1 we have sketched the band structure for a general PC where the BG is highlighted in yellow. The blue line is the full calculation of a band structure while the dashed green line is a Taylor expansion around the symmetry point. For the given band structure, the DOS for an ideal structure is shown in the middle panel. We can see how the expansion around the band edge (green dashed line) follows the ideal curve (blue line). In the right panel, we can see that the DOS is modified due to the contribution of a finite but small

γ. The effect of the small imaginary contribution γ is twofold: first, interference between the forward and backward wave is not completely destructive in the BG anymore [84], meaning that allowed states are created in the BG. The second effect is that due to the broadening of photonic states the DOS does not diverge at the band edge but it has a finite value, i.e. the Van Hove singularities are smeared out.

We can phenomenologically include all sources of structural and material imperfection by adding a small imaginary part ϵ'' to dielectric constant of PC [84]. When $\epsilon'' \ll \epsilon'$ we can apply perturbation theory [85, 15] for the electromagnetic eigenvalue problem. The perturbation theory is a class of mathematical techniques that allow to calculates the solution for a complex problem by "perturbing " solution of a simpler (idealized) problem.

We now consider the eigenvalue problem, i.e. eq. 2.18, for the PCW. By introducing ϵ'', we perturb $\omega(k)$ (eigenvalues) that results in a frequency shift

$$\Delta\omega = -\frac{\omega}{2}\frac{\langle \mathbf{E}|i\epsilon''|\mathbf{E}\rangle_V}{\langle \mathbf{E}|\epsilon'|\mathbf{E}\rangle} \tag{4.5}$$

Here, the integral in the numerator is restricted to the volume V containing ϵ'' (the dielectric material). We can rewrite the previous expression as

$$\Delta\omega = -i\frac{1}{2}\omega f\frac{\epsilon''}{\epsilon'} \tag{4.6}$$

where

$$f = \frac{\langle \mathbf{E}|\epsilon'|\mathbf{E}\rangle_V}{\langle \mathbf{E}|\epsilon'|\mathbf{E}\rangle} \tag{4.7}$$

is the filling fraction quantifying the energy in the dielectric [15]. Here, it is assumed that ϵ'' is in the dielectric. The dispersion curve $\omega(k)$ can be Taylor expanded in the proximity of k_0

$$\omega(k) \cong \omega_0 + v_{g,0}(k - k_0) + \beta_2(k - k_0)^2 + ... \tag{4.8}$$

where β_2 relates to the GVD. Ideally the excitation frequency ω is real while the Bloch wavevector $k = k' + ik''$ is complex. The effect of the small imaginary ϵ'' part is that in the guided band spatial damping is present.

From eq. 4.8 we can write $k(\omega)$ as a function of ω

$$k(\omega) = k_0 - \frac{v_{g,0}}{2\beta_2} \pm \frac{\sqrt{v_{g,0}^2 + 4\beta_2(\omega - \omega_0)}}{2\beta_2}. \tag{4.9}$$

When the Bloch wavevector is complex, v_g is defined as the derivative with respect to the real part of k, and we can write

$$v_g = \left(\mathrm{Re}\left\{ \frac{\partial k}{\partial \omega} \right\} \right)^{-1}. \tag{4.10}$$

We can now write the expression for v_g for a PCW using 4.6

$$v_g = \frac{\sqrt{v_{g,0}^4 + (2\beta_2\omega_0 \frac{\epsilon''}{\epsilon'})^2}}{\mathrm{Re}\left\{ \sqrt{v_{g,0}^4 + i2\beta_2\omega_0 \frac{\epsilon''}{\epsilon'}} \right\}}. \tag{4.11}$$

With these equations we can evaluate the effect of ϵ'' for a whole bandwidth. When we are at the band edge, the $v_{g,0} = 0$ property significantly simplifies the eq. 4.11 and we get

$$v_g = \sqrt{2\beta_2\omega_0 \frac{\epsilon''}{\epsilon'}}. \tag{4.12}$$

Here, we have assumed that $f = 1$. We can see from 4.12, in a very neat way, how v_g is compromised at the band edge. The GVD and ϵ'' are limiting factors of v_g. Even for very small amounts of ϵ'', v_g is seriously jeopardized at the band edge [84]. Equation 4.12 shows how v_g scales as a function of ϵ'', where the dependence is sublinear [84]. The sign of the imaginary part in the denominator does not influence v_g meaning that introduction of gain (negative ϵ'') has the same effect on the dispersion as loss. In the left panel of Fig 4.2, the spectrum of n_g for PCW is shown. In the right panel we can see that the scaling of n_g at the band edge is inversely proportional to $\sqrt{\epsilon''}$. Parameter details of the structure can be found in Paper A. From eq. 4.11 we can see that in the region

$$v_{g,0} \gg \sqrt{\alpha\omega_0 \frac{\epsilon''}{\epsilon'}}, \quad \text{or} \quad n_{g,0} \ll \sqrt{\frac{c^2}{\alpha\omega_0} \frac{\epsilon'}{\epsilon''}}, \tag{4.13}$$

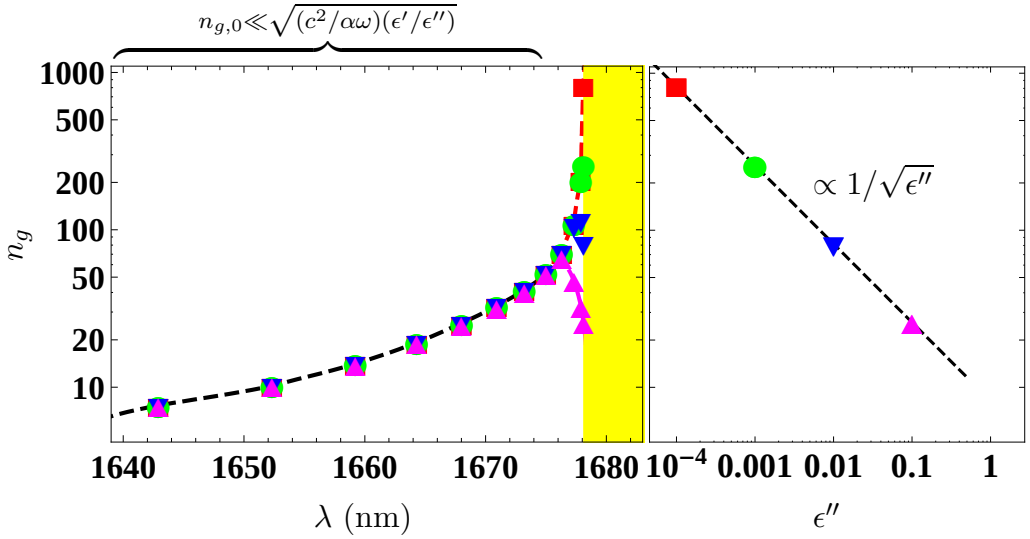

Figure 4.2 Group index for W1 waveguide in two-dimensional membrane PC with $\epsilon' = 12.1$. The left panel shows the group index versus wavelength for varying values of ϵ''. The right panel shows the group index at the band edge versus ϵ'', from Paper A.

the small imaginary part does not have any influence on n_g. The part of the dispersion curve that is close to band edge, on the other hand, is seriously affected by ϵ''. The electric field distribution of the slow light mode is spatially very spread in the PCW meaning that the mode interferes much more with any kind of imperfection. We can see from the right panel that for $\epsilon'' = (0.001, 0.01)$, n_g is in the range of $(100, 300)$; these are the max achievable n_g in PCW [80, 79]. The material loss in homogeneous silicon is $\epsilon''/\epsilon' \approx 10^{-9}$, and in comparison with the values considered in our calculation, we can conclude that major contribution to the limitation of the n_g must necessary be attributed to rather structural defects than intrinsic material absorption.

4.2 Group delay and group velocity limitations in CROWS

In the contrast with the previous section, losses in the CROW can be addressed in a closed analytical form. A CROWs dispersion relation $\omega(k)$ has a cosine dependence, which allows an easy analysis for infinite and ideal structures. Resonators constituting CROW in practical samples suffer from material and fabricational imperfection losses [38, 86, 87]. We can include the loss mechanism through the quality factor Q. Since the guiding mechanism in CROWs is based on the photons hopping from resonator to resonator, that is characterized by tunneling (hopping) time τ_t, the photon lifetime $\tau_p = Q/\Omega_0$ in the resonator has to be much bigger than τ_t in order to ensure guiding.

The complex frequency is defined as $\Omega = \Omega_0(1 + i/2Q)$ and we can work out the tight–binding model [39] that yields

$$\omega(k) = \Omega \left(1 + i\frac{1}{2Q}\right) \left(1 - \frac{\gamma}{2}\cos(ka)\right). \tag{4.14}$$

Now the coupling coefficient γ is a complex quantity, due to the fact that Ω is complex. But, the imaginary contribution is so small that it does not have any significant influence on the dispersion. We have introduced a complex resonator eigenfrequency in derivation of the CROW dispersion relation in the presence of loss. In the resonator, the field distribution is localized in space and oscillates in time. For that reason, loss is expressed as a decay in time. In the case of waveguides, the physical picture is different, the guiding mode is excited with a laser that has a well defined (real) frequency. A propagating field, in a waveguide, due to the losses decays spatially. By inverting eq. 4.14 we obtain k as a function of ω. Again, the Bloch wavevector $k = k' + ik''$ is a complex quantity that can be expressed in close form. We can calculate DOS as

$$\rho(\omega) = \frac{a}{\pi}\mathrm{Re}\left\{\frac{\partial k}{\partial \omega}\right\} \tag{4.15}$$

The density of states is normalized as $\rho\Omega_0$ meaning that we have DOS per resonator. In Fig. 4.3 we illustrate the complex photonic band structure and the corresponding DOS, for CROW with finite and infinite Q. In the

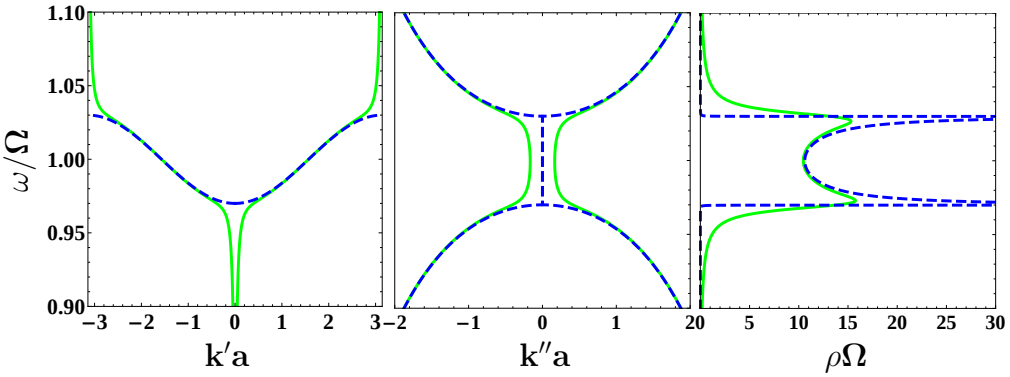

Figure 4.3 Complex dispersion relation for a CROW. Dashed lines are for $Q = \infty$ while solid lines correspond to $Q = 10^2$. The left panel shows the frequency ω versus the real part of the Bloch wave vector k', the middle panel shows the frequency ω versus the imaginary part of the Bloch wave vector k'', and the right panel shows the density-of-states ρ (per resonator), from paper C.

left panel where the real part of the band structure is shown, we have the standard cosine band for ideal structure (blue dashed line). When loss is introduced in the structure by a finite Q, we can observe how the dispersion curve close to the band edge bends (green line). The bending occurs due the introduction of Q and at a frequency corresponding to the inflection point where v_g reaches its maximum. In the middle panel, for frequencies with a guiding band in the ideal structure (green line), we observe $k''a = 0$. While k'' becomes finite and increases as we move out of the band. We can see that for non–ideal structure (green line), k'' has a finite value in the band meaning that propagation in the CROW will be accompanied with attenuation.The density of states is shown in the right panel, where introduction of Q smears out the Van Hove singularities (blue dashed lines). The finite value of the two peaks is proportional to the maximum n_g showing that SL is severely affected by Q at the band edges. Close to the band edge, the dispersion curve bends upward (downward) close to the symmetry point. In the bent region the dispersion curve is very steep meaning that v_g is superluminal. However, the special theory of relativity is not violated, because the definition of v_g in that region is not an appropriate definition for information transfer.

At the band center, the group velocity is $v_0 = \gamma a\Omega/2$ for an ideal structure

and if we compare it with v_g for structure with Q finite we have

$$\frac{v_g}{v_0} = 1 + \frac{1}{8}\frac{1}{\gamma^2 Q^2} + O(Q^{-4}) \tag{4.16}$$

We can see that at the band center, v_g is not affected by the Q as far as $\gamma Q \gg 1$. In the right panel of fig. 4.3, we can see that the DOS at the band center is unchanged. For practical devices, a pulse should have carrier frequency at the band center since v_g is not affected by Q and absence of GVD. The expression for v_g at the band edge is

$$\frac{v_g}{v_0} = \sqrt{\frac{2}{\gamma Q}} + O(Q^{-\frac{3}{2}}) \tag{4.17}$$

where we can see that at the band edge v_g is scaling quite unfavorable with Q. In connection with a limited v_g for PCW, we see that v_g scales with the same trend. The quality factor Q is proportional ϵ'/ϵ'' and eq.4.17 yields that in CROWs $v_g \propto \sqrt{\epsilon''}$, *i.e* the same general behavior as for PCWs.

Realistic structures are made up of a finite number N of resonators giving a length $L = Na$ of the waveguide. In this case v_g loses its meaning, since k is not continuous. It is more appropriate to use group delay τ_g as the quantity describing the light slow down. By increasing the number of resonators we increase the length meaning that τ_g increases. The amount of losses imposes a bound on the waveguide length $L \lesssim 1/\alpha$, where $\alpha = 2k''$. We get the expression

$$\tau_{max} \sim \frac{1}{v_g \alpha} \tag{4.18}$$

that is the upper limit of τ_g. We can expand in a Taylor series of $1/Q$ giving analytical expressions of α and v_g, leading to

$$\tau_{max} \sim \frac{Q}{\Omega_0} + O(Q^{-1}) = \tau_p + O(Q^{-1}). \tag{4.19}$$

Equation. 4.19 gives an important insight that maximum τ_g is limited by the photon lifetime in the single resonators. But in comparison to the single resonator the CROW offers a larger bandwidth. By reducing v_g, the interaction

time increases meaning that loss is enhanced. If a pulse is propagating slower it gets more attenuated. The issue of losses and v_g has to be taken on the same footing to have full advantage of CROW.

Deviations in the geometrical shape of the individual resonator, due to the fabricational processes, translate into fluctuations of Ω and γ. In the SL regime, we know that structures are extremely sensitive to imperfections, meaning that n_g will drop significantly even for small structural defects [8, 88]. Another problem that occurs with disorder (fluctuations), is that Anderson localization occurs [89, 88, 90]. The field will be localized somewhere within the CROW. Where the localized field has spatial distribution that decays exponentially. The strength of localization is characterized by the localization length l_l. If the structure length L is longer than l_l then the field cannot be coupled out from the structure. The disorder strength has to be smaller than the energy separation between two neighboring energy levels (the separation between two successive eigenvalues) in order [38] to have states (fields) that extend in the whole waveguide. The transmission through the CROW of length L is parametrized by

$$T(\omega) = \exp\left(-\frac{\xi(\omega)}{L}\right) \tag{4.20}$$

where $\xi(\omega)$ is the characteristic length and it takes into account the effects of disorder and losses in the structure. The maximal length of the structure has to be $\xi(\omega)$ otherwise transmission through the structure is inefficient. The maximal delay that can be achieved in the CROW is then

$$\tau_{max}(\omega) = \frac{\xi(\omega)}{v_g(\omega)} = -\pi\rho(\omega)\ln T(\omega). \tag{4.21}$$

In order to calculate τ_{max} in the presence of the disorder we implement the Green function method suggested by Datta [91, 92]. A segment of the disordered waveguide of N elements is coupled to an infinite ideal CROW by self energy coefficient $\mathbf{\Sigma}(\omega)$ that results in a $N \times N$ Green matrix

$$\mathcal{G}(\omega) = [\omega\mathbf{I} - \mathbf{H} - \mathbf{\Sigma}(\omega)]^{-1} \tag{4.22}$$

where **I** is the identity matrix, and **H** the tight-binding Hamiltonian . For CROW made of N elements we can set up a Hamiltonian matrix **H**

$$H_{ii} = \Omega_0 \left(1 + \sigma_\Omega + i\frac{1}{2Q}\right)$$
$$H_{ii\pm1} = \Omega_0(-\gamma + \sigma_\gamma). \tag{4.23}$$

Disorder is introduced by adding the Gaussian distribution with standard deviation σ_Ω (σ_γ) to diagonal (off–diagonal) elements of the matrix. The amount of σ indicates the strength of the disorder in the structure. We will for simplicity assume that linewidth is not subject to deviations, meaning that Q will remain constant.

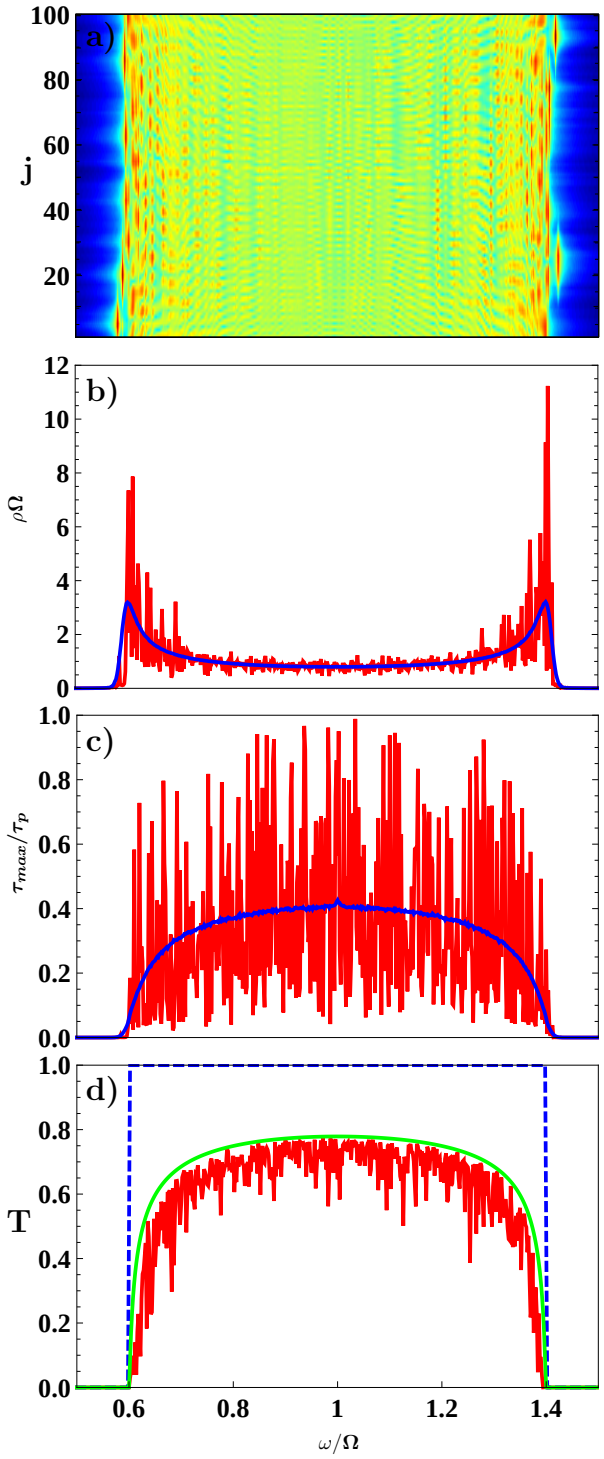

Figure 4.4 Properties of a disordered CROW, with blue lines indicating ensemble-averaged properties while the red lines illustrate the results for a particular realization of the disorder, thus emphasizing pronounced CROW-to-CROW fluctuations. Panel (a) shows the local DOS ρ_j for a particular realization of the disorder and panel (b) shows the corresponding results for the total DOS ρ (per resonator). Panel (c) shows the maximal group delay $\tau_{\max}$. Panel (d) shows results for the transmission. For comparison, the dashed line shows the unity transmission for an ideal crow, while the green line is for a non-disordered CROW, but with a finite Q, from paper C.

In the panel a) of Fig. 4.4 the local DOS is shown, in the map we can see how states are distributed locally in the CROW. We can see that, states are very extended in the center of the band . But in the region close to the band edge the red spots indicate spatially localized modes. That is the indication of Anderson localized modes, that occur due to the strong interference effect. We show in the panel b) the DOS for one realization of the ensemble (red line) and the average DOS (blue line) of the ensemble. For different realizations the sample to sample deviation of the DOS is huge. The averaging smears out Van Hove singularities in the DOS. In this model, losses and disorder have been included, meaning that the overall effect on smearing of the average DOS is even stronger. The maximum achievable delay for a CROW with finite Q, is τ_p. For that reason, we have normalized τ_{max} with respect to τ_p. We can see that average τ_{max} (blue line) is much lower than τ_p. Again, the deviation of one realization (red line) is huge in respect to the average and τ_{max}/τ_p is always below 1. The presence of the disorder makes the design of the CROW very challenging, because small deviations in the geometry cause big fluctuations in important design parameters. The panel d) shows $T(\omega)$, in an ideal CROW (blue dashed line) where transmission over the whole bandwidth is 1. With finite Q, transmission (green line) has been decreased, and has a constant value around center band. But as we approach the band edge, we can see how $T(\omega)$ is decreasing. The decay of $T(\omega)$ is due to SL enhancement of attenuation that becomes significant in the vicinity of band edges. The presence of disorder, together with losses, makes things even worse; fluctuations in transmission spectrum (red line) occur and max T is limited in the finite Q case.

An interesting interplay between loss (finite Q) and disorder can be observed if we look at fig. 4.5. We show τ_{max}/τ_p at the band center as a function of disorder strength σ, for different values of Q. The highest $Q = 10^6$ is the one that decays faster with the increase of σ meaning that it is extremely sensitive to small disorder. On the other hand, the structure with the lowest considered $Q = 10^2$ shows that it is robust with respect to the influence of disorder. High Q means that the electromagnetic field is well confined within the resonator and the evanescent tails overlap of the two neighboring

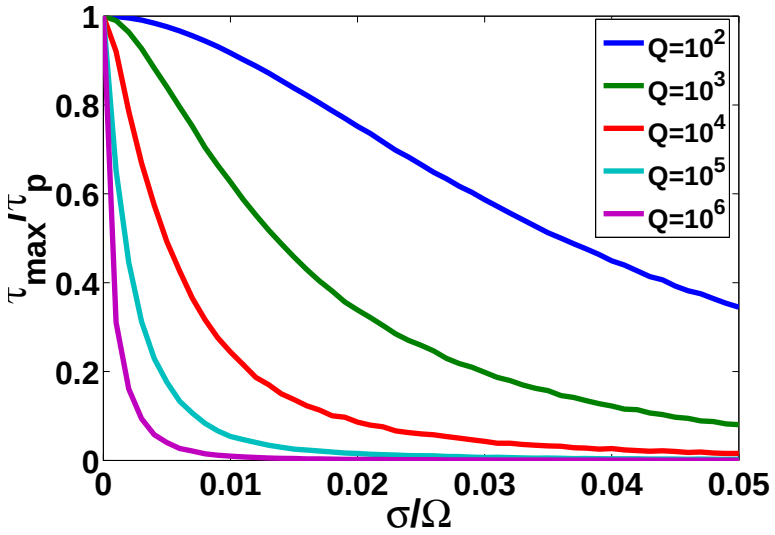

Figure 4.5 Maximal group delay τ_{max} at band center versus disorder strength σ, from paper C.

resonators is very small and sensitive to the smallest imperfections. For a low Q, field overlap does not depend significantly on disorder.

Material and structural imperfections in a CROW have strong implications on light propagation. Just by the presence of a finite Q, the minimum v_g at the band edge is seriously compromised. Due to the disorder the SL region is susceptible to localization and strong fluctuation in waveguide parameters from sample to sample occurs. All imperfections in the SL region are very pronounced and for that reason design of CROW is quite a challenge.

4.3 Group index limitations in HCF

As the last example, we briefly discuss the effect of losses on HCF with a SL mode. The group index of such a fiber is also subjected to limitations due to material and structural imperfections. In comparison with the previous section where we used analytical methods to evaluate the effect of losses in PCW and CROW, we would like to point out that a full numerical calculation has been performed for HCF. Waveguiding and light confinement in the core in this fiber rely on the periodic structure. It has been suggested [93] that

the number of rings should be at least 17 in order to reduce leakage losses to values of attenuation in step index fibers. Such a big number of rings yields an extremely expensive computational domain, in terms of memory and computational time. As a good compromise between computational domain and light confinement, we decided to put 6 rings around the core. Here we solve the full electromagnetical (eigenvalue) problem with a finite elements method (FEM) and an absorptive medium in the core. This allows us to calculate the complex dispersion, $\beta(\omega) = \beta'(\omega) + i\beta''(\omega)$ of the HCF and n_g by deriving numerically $\beta'(\omega)$.

One of the practical limitations for such type of fiber is also the fact that the SL mode has a very complicated field distribution which means that in/out coupling could be very challenging, since there will be big mode mismatch with modes in the step index fibers.

From Fig. 4.6 we can see the spectrum of n_g for the different values of n''(0.001,005,0.01). The maximum achievable n_g depends strongly on n''. We

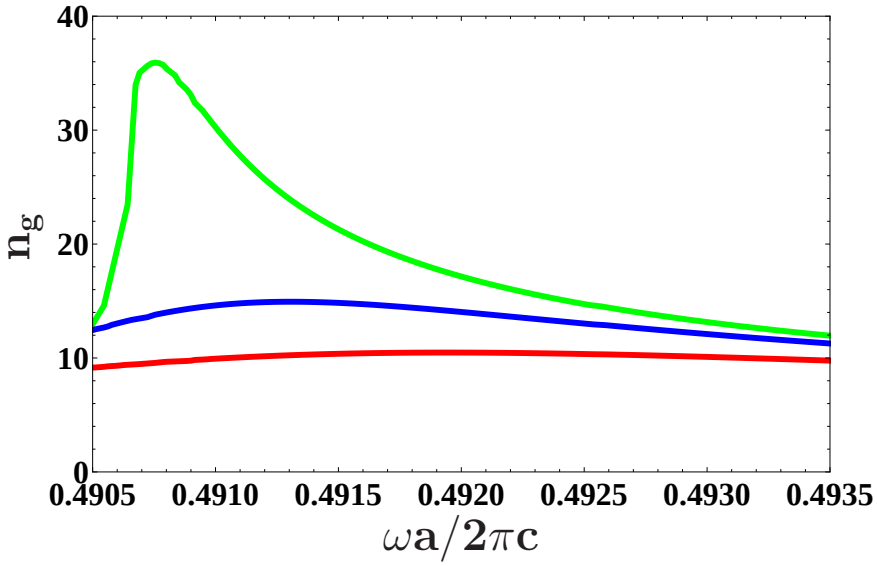

Figure 4.6 Group index spectrum for three different values of n" (0.001, 0.005, 0.01). from paper D.

should emphasize that this limitation is more severe than in previous cases, because of presence of the leakage loss in the transversal plane. We can see very similar trends in the scaling of the n_g vs. n'' as in the previous cases

of PCWs and CROWs. The effect of the imaginary part on the dispersion curve is very a general feature for periodic guiding structure.

5

Enhanced light-matter interaction

Key results from papers D and E are summarized here. In the first section we explore loss enhancement determine how loss enhancement is related to slow light. As a practical example we have analyzed a hollow core photonic crystal fiber (HCF) in section 5.1 . Gain enhancement is analyzed in the section 5.2, and we highlight similarities of gain and losses in a terms of enhancement and limitations of SL. As a practical example we have studied three important periodic structures, with numerical and analytical methods.

5.1 Loss

Due to weak light–matter interaction in on–chip optical devices it is necessary to have long interaction times $\tau_i = L/v_g = n_g L/c$, where L is the device length. Since the structure length cannot be changed, in order to increase τ_i it is necessary to slow down the speed of light. By doing so, τ_i will linearly increase with n_g. Periodic structures have a strong dispersion which becomes almost flat in the vicinity of the band edge. Therefore, light–matter interaction is enhanced in this region due to high n_g. We can explain heuristically the enhancement in periodic structures using the example of a Bragg Stack (BS). When light propagates thorough a BS it bounces back and forth due to the periodicity of the refractive index. This multiple reflection increases the optical path, meaning that τ_i becomes much longer than in a homogeneous medium. The light thus interacts much longer with the medium than in the homogeneous case and therefore gives rise to enhancement. For a BS

infiltrated with absorptive gas, it has been shown experimentally that SL enhances absorption [94]. Absorption of light is described by the Beer–Lambert law

$$I = I_0 e^{-\alpha L} = I_0 e^{-\Gamma \alpha_l L}, \tag{5.1}$$

where I_0 is the light intensity, $\alpha_l = 2k''$ is the absorption coefficient and Γ a dimensionless parameter that takes into account enhancement of light–matter interaction [11]. In homogeneous media, Γ_0 is close to unity while in periodic media Γ_0 can be quite large [11, 70]. Absorption in periodic media is given by the imaginary part ϵ'' that gives complex dielectric constants $\epsilon = \epsilon' + i\epsilon''$ for eq. 2.18. Again as in Section 4.1, we assume that absorption is very week, $\epsilon'' \ll \epsilon'$, which allows us to use perturbation theory [15, 85] to evaluate the overall absorption in the periodic media. Assuming that the excitation frequency ω_0 is fixed, the change due to ϵ'' occurs in wavevector; in other words ϵ'' causes an imaginary shift $i\Delta k''$. We can express $\Delta k''$ using eq. 4.6 in the following way

$$\Delta k'' = \frac{\partial k'}{\partial \omega} \Delta\omega = \frac{1}{v_g} f \omega_0 \frac{\epsilon''}{2\epsilon'}. \tag{5.2}$$

The absorption coefficient in periodic media is $\alpha_p = 2\Delta k''$, so we can write

$$\alpha_p = \left(\frac{\omega_0}{c}\right) n_g f \frac{\epsilon''}{\epsilon'} = 2k_0 n'' f \frac{n_g}{n'}. \tag{5.3}$$

While for homogeneous media, absorption is

$$\alpha_l = 2k_0 n'' \tag{5.4}$$

by taking ratio of α_p to α_l we get the enhancement factor

$$\Gamma_0 = f \frac{n_g}{n'}. \tag{5.5}$$

Equation 5.5 shows that Γ_0 scales linearly with n_g, meaning that SL increases τ_i. The filling factor f has to be as close as possible to 1 in order to take full advantage of the enhancement. If n_g is very high but the confinement is very

weak (low f) in the waveguide, then there wont be any enhancement because the contribution of high n_g is overcome by the low f [29]. In Chapter 4, we showed how a small imaginary part affects SL. If we want to calculate Γ_0 self–consistently we have to include the effect of ϵ'' on n_g meaning that enhancement Γ_0 will be limited due to saturation of n_g.

Now we will show an example of the enhancement of absorption in HCF. We have performed full FEM calculation for this problem, where the core has been infiltrated with weakly absorbing gas. In the left panel of fig. 5.1 we show the real part of the dispersion relation $\beta'(\omega)a/(2\pi c)$ for 4 different values of n''. There are 4 curves in the left panel and we can see that even

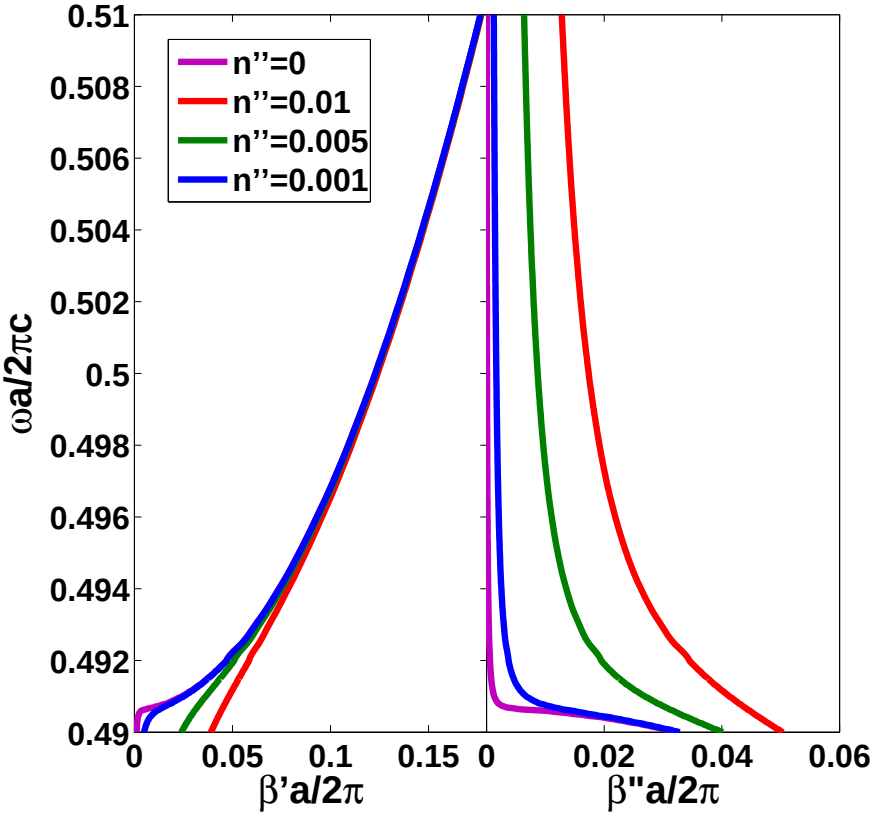

Figure 5.1 Complex dispersion relation for the hollow core fiber being infiltrated by an absorbing gas with $n = n' + in''$ with $n' = 1$ and n'' ranging from 0 to 0.01. The left panel shows the dispersion while the right panel shows the corresponding absorption in dependence of the frequency (vertical axis), from paper D.

for a lossless HCF (blue line) close to the band edge, the dispersion curve

bends down. Due to the finite periodic environment (6 rings) around the core, there is a small leakage of energy. For this reason, the dispersion curve bends and become very steep in the vicinity of $\beta'' = 0$. We can see that for the other 3 curves as n'' is increasing bending becomes more and more prominent. In the right panel, the imaginary part of the dispersion relation $\beta''(\omega)a/(2\pi c)$ is shown. When $n'' = 0$ in the HCF, we can see that the loss in the whole band is negligible. But for finite n'', it is clear that absorption in whole guiding band increases with increased n''. In the vicinity of the band edge β'' becomes quite large and absorption is enhanced.

It is necessary to distinguish between two sources of loss in the HCF in order to properly evaluate the enhancement. There are losses due to the energy leakage and losses that are intentionally introduced in the structure (by the absorbing gas). We are interested in evaluating the enhancement of the gas absorption

$$\Gamma = \frac{\beta'' - \beta''(n'' \to 0)}{n''}, \tag{5.6}$$

while neglecting leakage losses. For that reason, the influence of finite effects is removed by applying eq. 5.6.The left panel of fig. 5.2 shows the spectrum of Γ for the HCF and ithe right panel shows the spectrum of n_g. The enhancement follows nicely the behavior of n_g; where for $n'' = 0.001$ we can see clearly the proportionality between the two curves. Small discrepancies between the curves are still present, but they are due to numerical artifacts. For the two curves that correspond to values $n'' = (0.01, 0.005)$, we can see that the maximum Γ_{max} is 4 and 6 respectively. Γ and n_g do not have the same qualitative behavior, because for the corresponding values of n'' we are on the limit of validity of the perturbation theory. Nevertheless, enhancement is still present and is due to the SL effect. But, there is clear evidence that by increasing absorption, n_g saturates; and as a consequence limits the enhancement.

In fig 5.3 we summarize the previous discussion by showing $\Gamma_{\max}$ as a function of n''. We have performed calculation for additional two values of n'' that haven't been included in the previous figures. We can observe how $\Gamma_{\max}$ scales with n''. This plot illustrates clearly that $\Gamma_{\max}$ increases

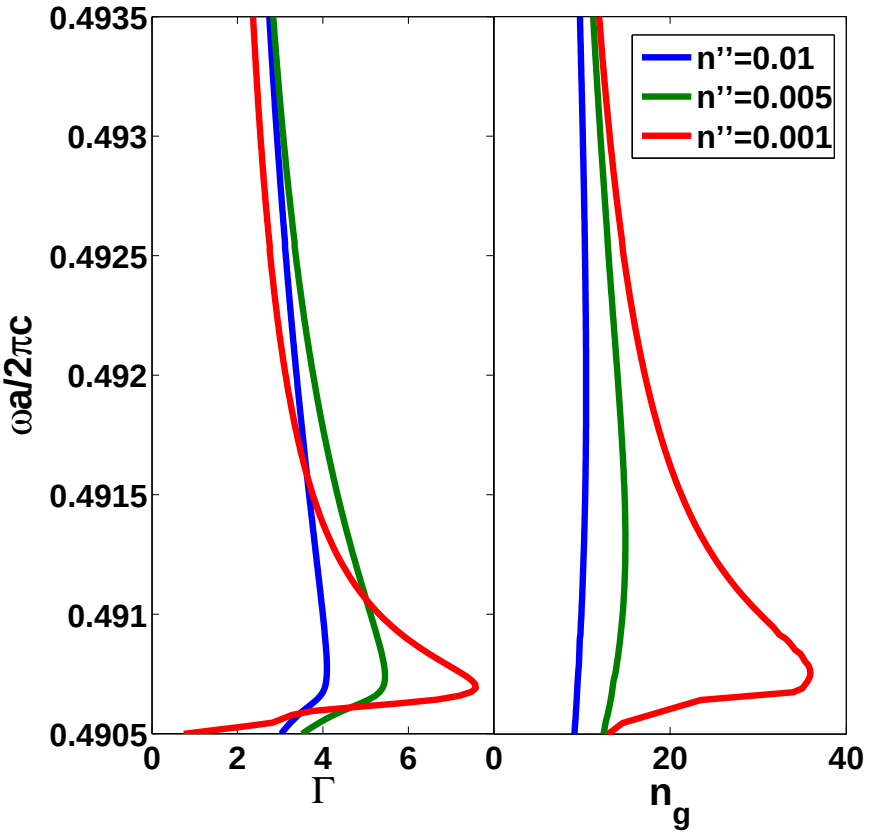

Figure 5.2 Comparison of the absorption enhancement factor (left panel) and the group index (right panel), both derived from the results in Fig. 5.1. For the absorbing gas, n'' is varied in the range from 0.001 to 0.01. ,from paper D.

as n'' is diminished. The small amount of absorption doesn't perturb the dispersion curve strongly; meaning that high values of n_g are obtained. High absorption strongly jeopardizes n_g which results in the suppression of Γ. Even though HCF is a translationally invariant structure, the dispersion and tight confinement are consequences of periodicity in the transversal plane. For that reason, HCF shows the same physical properties as other periodical structures when absorption and n_g play in a concert. The enhancement is promoted by SL, but only for weakly absorbing media, otherwise v_g will saturate and the effect will disappear.

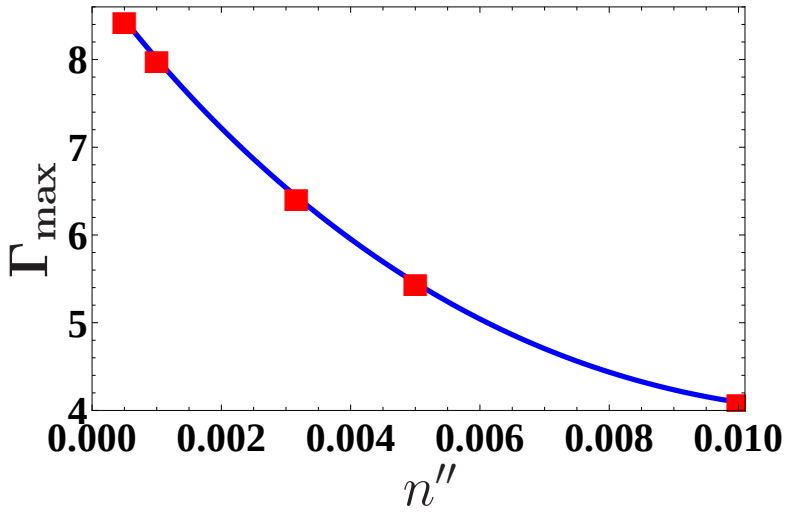

Figure 5.3 The maximal absorption enhancement factor $\Gamma_{\max}$ versus intrinsic gas absorption n'' for the infiltrated gas, from paper D.

5.2 Gain

Slow light appears to be a solution for various photonic devices in which it is necessary to maximize otherwise weak light-mater interactions. Introducing active media in nanophotonic structures is of great technological and fundamental interest. Loss compensation in metamaterials and plasmonics is addressed by the introduction of active media [95, 96, 97]. Devices such as amplifiers [98], low–threshold laser [99], mode–lock lasers [100] are structures that take great advantage of gain in periodic environment. The enhancement of gain has been theoretically studied Dowling *et al.* [64] for 1D PCs, while 2D and 3D structures have been studied by various other groups [54, 98, 101]. We have seen from the previous example, that the absorption and dispersion of periodic media are interdependent. By changing the sign of ϵ'' in the complex dielectric constant, we can introduce gain in periodic media. Perturbative analysis, from the previous section, can be performed in the same manner for homogeneous gain. The limiting effect on v_g is the same as in the case of losses. The fundamental difference however is that a signal propagating through periodic media with gain, will be amplified; while in the presence of absorption, the signal is attenuated. It is suggested in [2]

that gain is independent of structural dispersion. This is true for a small amount of introduced gain which present a beneficial effect of SL, namely, that the effective gain g_{eff} is enhanced. By exploring three important structures: CROW, BS and PCW, we will explain with more detail the effect of gain enhancement and its limitations.

In CROW, the gain can be introduced by adding a small imaginary part g_0 to the frequency.

$$\omega(k) = \Omega\,(1 - ig_0)\,[1 - \gamma\cos(ka)]. \tag{5.7}$$

We can see that eq. 5.7 is the same as eq. 4.14 where only the sign of the imaginary part in the expression has been changed. The calculation of the dispersion relation yields the same curves for complex dispersion and DOS, as in fig 4.3. Even though all curves look the same, there is a crucial difference with the imaginary part of the dispersion curve k'. Instead of losses, therefore k'' now accounts for amplification. The real part of the dispersion curve will bend due to the introduction of g_0. We know from section 4.2 that losses will introduce broadening of DOS. Since bending of the real part is identical as in the lossy case, the effect of gain on DOS is same as in the presence of losses. Intuitively, there might be the wrong expectation that gain will just sharpen the DOS. In fig. 5.4, we put together three curves representing: lossy ($-g_0$), gain (g_0) and ideal structure ($g_0 = 0$). We can see that gain and loss with the same absolute value have a similar effect on the DOS. From this example we can see that gain enhancement depends strongly on the amount of introduced homogeneous gain. Large amounts of g_0 saturate the SL effect and as a consequence the enhancement will be suppressed. However, if small amounts of g_0 is introduced then we will still have high n_g which will promote enhancement. With the next examples, we will see that the effect is indeed a general property of periodic structures.

A Bragg stack is a periodic 1D PC consisting of alternating layers of thickness a_1 and a_2, with dielectric constants ϵ_1 and ϵ_2. The dispersion

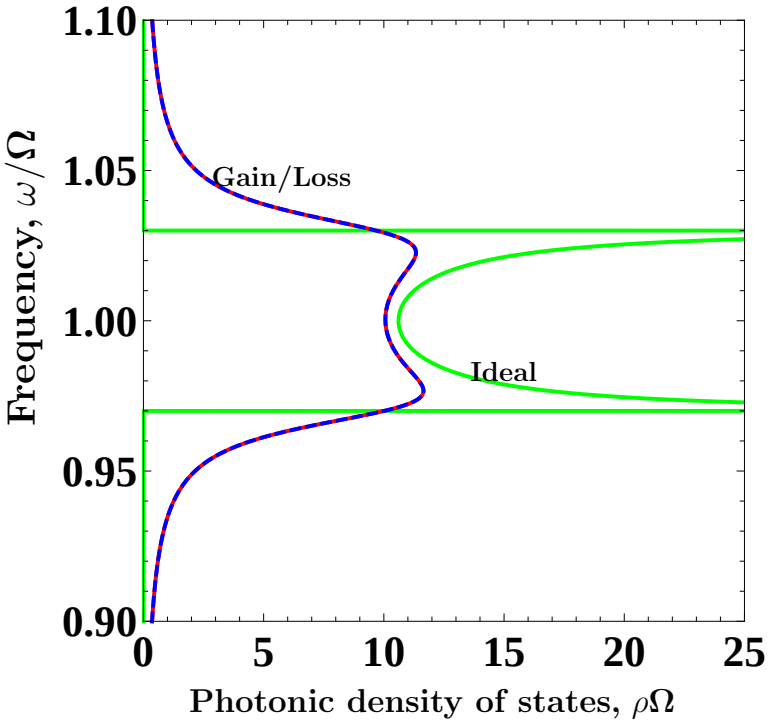

Figure 5.4 Photonic density of states (per resonator) ρ (lower horizontal axis) and group index n_g (upper horizontal axis) versus frequency ω, for a CROW with $\gamma = 0.03$. For passive resonators with $g_0 = 0$, van Hove singularities appear at the band edges (green line). For $g_0 = \pm 0.01$, gain (blue-dashed line) or an equivalent loss (red line) cause a similar smearing of the singularities, from Paper E.

relation for BS can be calculated in a closed form [64] and is given by

$$\begin{aligned} \cos(ka) &= \cos\left(\sqrt{\epsilon_1}a_1\frac{\omega}{c}\right)\cos\left(\sqrt{\epsilon_2}a_2\frac{\omega}{c}\right) \\ &\quad + \frac{\epsilon_1+\epsilon_2}{\sqrt{\epsilon_1}\sqrt{\epsilon_2}}\sin\left(\sqrt{\epsilon_1}a_1\frac{\omega}{c}\right)\sin\left(\sqrt{\epsilon_2}a_2\frac{\omega}{c}\right) \end{aligned} \tag{5.8}$$

where $a = a_1 + a_2$ is the lattice constant. In this case the loss/gain can be introduced by an imaginary part ϵ''. For simplicity we have introduced the same ϵ'' in both layers.

In panel a), from fig. 5.5 we have the real part of the dispersion relation where yellow indicates the band gaps. We can see that in the presence of the moderate loss/gain (red line) the effect of the BG disappears. Forward and backward propagating waves experience different amplification (or attenua-

tion) and thereby have different amplitudes. Due to this reason, destructive interference is not complete meaning that the BG effect disappears. Panel b) illustrates the imaginary part of the dispersion relation. For the ideal structure (green line) we have a finite imaginary wavevector k'' in the BG region and zero out of the BG. When moderate gain/loss is introduced we can see that k'' has a finite value outside the BG meaning that in the guided band, gain/loss is present. Close to the band edge the gain/loss is enhanced, but it is clear that the effect is not infinite. The finite value of k' indicates that due to the introduction of ϵ'', we bound the maximum value of n_g which produces a limitation of the enhancement. As a limiting case we can introduce extremely large ϵ''. The effect is that any indication of a BG completely vanishes, the BS responds as a homogeneous material(blue line).

As a last example, we will analyze a PCW when a homogeneous gain is introduced. The geometric complexity requires a full numerical treatment. We used FEM, with a super cell approach with boundary conditions fulfilling Bloch wave conditions with complex wave number k in the direction of the waveguide and simple periodic conditions in the transverse direction [102]. The gain is introduced by adding a small imaginary ϵ''. Like in the two previous cases, n_g is affected by the amount of the ϵ'' while the sign doesn't influence the effect.

For practical devices, such as amplifiers, homogeneous gain is defined as $g_0 = 2n''(\omega/c)$, where $n = \sqrt{\epsilon} = n' + in''$ is the complex refractive index. With an imaginary part of the dispersion we can evaluate the effective gain $g_{\text{eff}} = 2k''$ in a PCW. We know from eq. 4.11 that n_g at the band edge is proportional to $g_0^{-1/2}$, while $g_{\text{eff}} \propto g_0 n_g(g_0)$. This yields

$$g_{\text{eff}} \propto g_0^{1/2}. \tag{5.9}$$

We have also evaluated Γ and g_{eff} for 2D PCW with $\epsilon' = 12.1$; while gain is introduced by ϵ''. The results are illustrated in fig 5.6 where g_{eff} and g_0 are normalized with respect to a. Γ and g_{eff} are evaluated at the frequency ω^* that is slightly detuned from the bend edge. Due to that reason n_g has a small constant under the square root (eq. 4.11) meaning that $n_g \propto$

$(const. + g_0)^{-1/2}$. The g_{eff} scales with the square root law of g_0 at the band edge (red line). This expression is very important because it takes into account the limitations introduced in n_g when we are evaluating Γ. By doing so, the effect on enhancement limitation is calculates self consistently. In the inset of fig. 5.6 we can see the deviation from square root law for small values of g_0, in log–log scale, because of slight detuning from band edge frequency . For a bigger values of g_0, calculated values (red dots) match nicely with a simple square root. On the left hand axis we have Γ. The blue line clearly shows that for very small values of g_0 we have a big enhancement. When values of g_0 increases the enhancement decreases.

Surface roughness, deviations in hole position and size, finite structure effects, material losses *etc.* are the main sources of limitation in passive PCWs. We have seen from statistical studies, done for CROWs, that averaging of disorder effects result in broadening of DOS. With more advanced methods [103, 78] for PCWs, the averaging effect on DOS has the same effect. Since the overall average effect of weak disorder could be mapped in ϵ'', it appears that if we are able to introduce homogeneous gain, with respective $-\epsilon''$ we could compensate losses and recover the ideal n_g completely. However, it is not clear whether we would compensate losses or introduced even more broadening to the structure.

To conclude, we have studied 3 different periodic structures that are of significant technological and fundamental interest. Each structure has strong dispersive properties due to the periodicity. We have explored the effect of gain enhancement due to the SL effect with analytical and full numerical calculations. BS and CROW have closed form solutions where the enhancement and gain back-action on dispersion are treated on the same footing. On the other hand, the electromagnetical problem has been solved self–consistently using a numerical method. Comparing closed form, perturbative and numerical results show the same qualitative behavior for the aforementioned structure. The effect of gain/loss on v_g and therefore on enhancement is a very general feature for any periodic structures. Whenever we want to take advantage of gain enhancement it is important to use active material with small gain (*e.g* layer of quantum dots). Otherwise, if gain is too large, the

n_g will be compromised resulting in less enhancement.

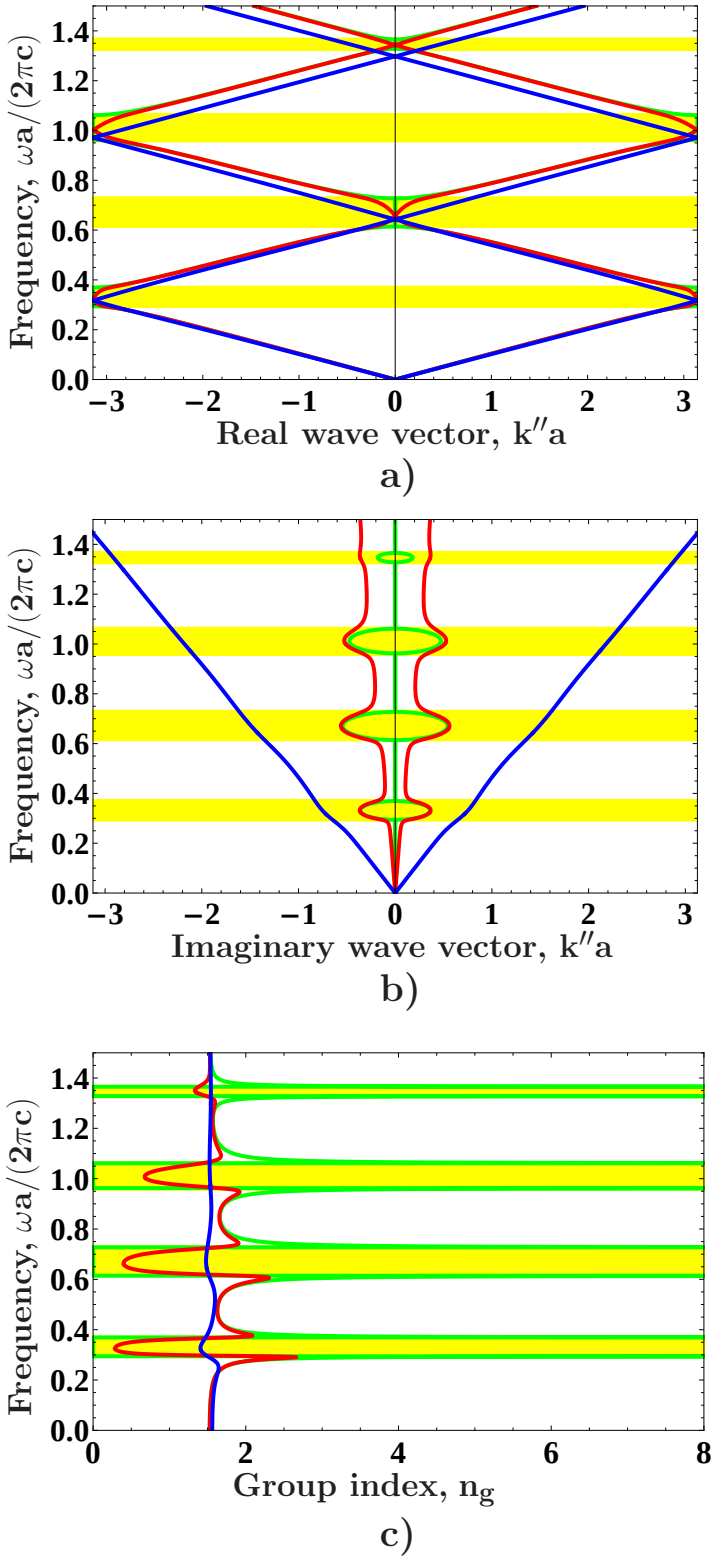

Figure 5.5 a) Real part k' (horizontal axis) of the Bloch vector as a function of frequency ω (vertical axis), b) Imaginary part of the Bloch vector k'' (horizontal axis) versus frequency ω (vertical axis) and c) The group index n_g (horizontal axis) versus frequency ω. The green line represent the ideal structure while the red line show the effect of gain/loss, the blue line shows the effect of exaggerated loss/gain.

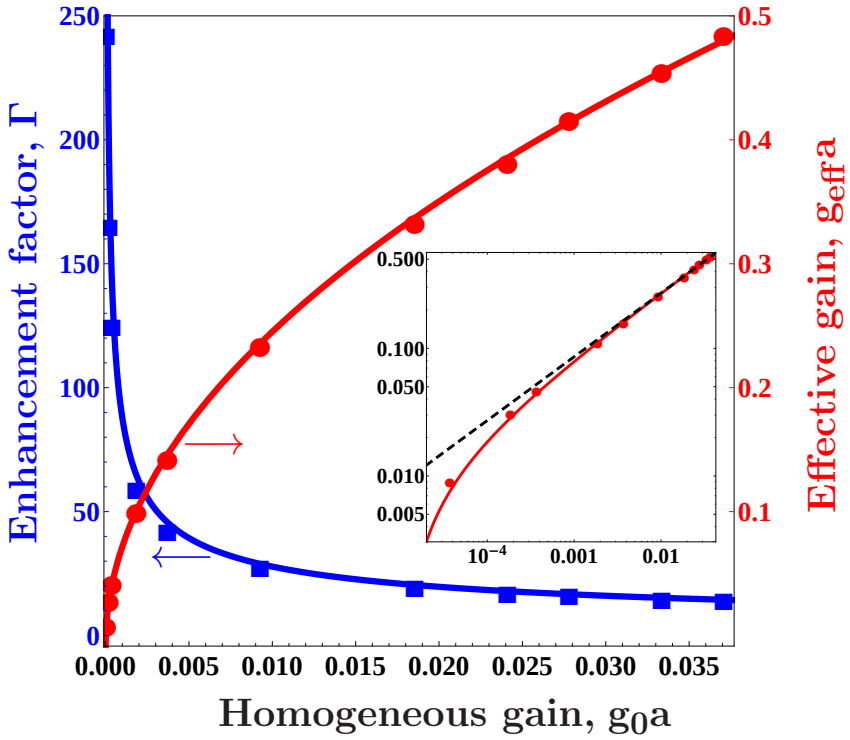

Figure 5.6 Slow-light enhanced gain g_{eff} (right-hand axis) versus homogeneous gain g_0, evaluated at ω^* where the group index is initially maximal. The red solid line shows a fit to the anticipated square-root dependence, (see eq. 5.9), while the inset (log-log scale) exhibits minor quantitative deviations from a strict square-root dependence (dashed black line) due to a slight detuning from the band-edge singularity, see discussion in text, from Paper E.

6

Conclusions & Outlook

In this thesis important aspects of the limitation of slow light (SL) and enhancement of light–matter interaction in periodic structures have been covered.

In the first part of my PhD, I have been looking into limitations of SL in PC waveguides (PCW) and coupled resonator optical waveguides (CROW). For an ideal PCW, in proximity of the band edge the speed of light can be drastically slowed down and at the band edge, light can formally be stopped. However, in experiments, it has never been possible to attain a group index n_g higher than 300 [79, 80]. Fabricated PCWs are affected by numerous imperfections like: surface roughness, material absorption, scattering losses, finite size effects and radiation losses. All those imperfections decrease the amount of the transmitted energy through the structure, but what is more important the SL properties are severely affected [9]. Very detailed studies on every single effect of imperfection require complex analytical methods and very demanding simulation efforts. By making assumption that imperfection can be translated into a small imaginary part of dielectric constant then good insight on limitation of SL, in perturbative regime, can be obtained very easily. With our approach, we can understand what are the major sources of limitation of SL in PCW and how the maximum n_g scales with the overall effect of imperfections. For a CROW, we have performed an analysis where simple homogeneous loss was introduced in an ideal structure. The advantage of studying the CROW is that dispersion even in a lossy case can be calculated in a closed form. The scaling law for v_g in a CROW has the same

qualitative behavior as in the PCW. The CROW has been studied in more detail where disorder is added to an already lossy structure. In that situation, we could see that SL properties has strong fluctuations that make device design very challenging. Furthermore, if disorder is very strong, the SL regime can lead to localization effects that can suppress transmission completely. Disorder and loss are inherent properties of every periodic structure, and no matter how small they are, implications on SL are strong. As another example, a photonic crystal fiber (HCF) is studied with a full numerical method where we found that limitation on SL follows the same scaling law as in the previous two cases. Addressing the problem of limitation of SL with numerical and analytical methods for 3 different periodic structures we conclude that the effects of small imperfections on SL is a general property of periodic structures.

On–chip–optical devices should offer the same or better properties in respect to the bigger devices and at the same time have much smaller size. By shrinking the length of *e.g.* amplifiers, then overall amplification decreases. It is necessary to use very long device that is in contrast with miniaturization requirements. SL in structured dielectric media can solve a problem of weak light-matter interaction. In a very simple picture, due to the slow propagation of light the interaction time in the medium is longer and that results in enhanced light–matter interaction. If dispersive properties were independent of loss/gain then enhancement would only depend on the size of n_g. However, loss and gain can also be understood as a perturbation of the dielectric constant of an ideal structure meaning that it is important to take into account limiting effect on v_g. An interesting structure for gas sensing applications, HCF is analyzed in detail, where the peculiarities of interplay of losses and dispersion are discussed. PCW, CROW and Bragg stack are studied within the context of gain enhancement with numerical and analytical methods. All 4 aforementioned structures can enhance light-matter interaction, but only for a weak gain/loss.

Regardless of the fundamental difference between loss and gain on signal amplitude, the limiting effect on the SL is the same. For very weak light-matter interaction, dispersion is not severely affected meaning that high n_g

can be achieved. Since the enhancement is directly proportional to n_g we can greatly enhance very low gain/loss. However, if the amount of loss/gain is large, then v_g will be completely jeopardized and therefore enhancement will disappear. Extremely short amplifiers can not be constructed by using a periodic structures, but in the case of very weakly amplifying media (*e.g.* quantum dots layer), the effect of SL is still beneficial, where the decent increase of effective gain can be expected.

We have used a phenomenological approach in this thesis in order to address the problem of loss/gain limitation of enhancement. However, we get a good insight in the very fundamental property for any periodic structure. We can predict the maximum enhancement for a given structure in the linear regime, where only a small perturbation to the ideal structure is introduced by gain/loss. But we would like to emphasize that our results and analysis is valid only in the perturbative regime. For the strong disorder regime, the perturbative approach can not be used meaning that detailed numerical analysis are necessary. Using finite difference time domain coupled to rate equations would be definitely interesting approach in order to address the more complete picture of gain enhancement in real structures. The nonlinear processes have a double advantage in the SL regime: longer interaction time and scaling of the nonlinear constant with n_g^{n-1}, where n is the power of the nonlinear process (such as Kerr nonlinearity where $n = 3$) [69]. It would be very interesting to study the effect of enhancement in nonlinear regime and, understand if it is subjected to other kind of limitations. Since is not quite clear how combined effects of disorder and gain in periodic media will affect structural dispersion of PC It would be important to understand if gain could has any beneficial effect in the SL propagation regime or SL properties would be further compromised by introduction of gain.

Bibliography

[1] Gauthier, D. J. Slow light brings faster communication. *Physics Word* 30 (2005).

[2] Krauss, T. F. Slow light in photonic crystal waveguides. *J. Phys. D-Appl. Phys.* **40**, 2666 – 2670 (2007).

[3] Baba, T. Slow light in photonic crystals. *Nat. Photon.* **2**, 465 – 473 (2008).

[4] Baba, T. Photonic crystals: Remember the light. *Nat. Photonics* **1**, 11–12 (2007).

[5] Hau, L., Harris, S. E., Dutton, Z. & Behroozi, C. Light speed reduction to 17 metres per second in an ultracold atomic gas. *Nature* **397**, 594–598 (1999).

[6] Bigelow, M. S., Lepeshkin, N. N. & Boyd, R. W. Superluminal and slow light propagation in a room-temperature solid. *Science* **301**, 200–202 (2003).

[7] Thevenaz, L. Slow and fast light in optical fibres. *Nat. Photonics* **2**, 474–481 (2008).

[8] Patterson, M. *et al.* Disorder-induced coherent scattering in slow-light photonic crystal waveguides. *Phys. Rev. Lett.* **102**, 253903 (2009).

[9] Pedersen, J. G., Xiao, S. & Mortensen, N. A. Limits of slow light in photonic crystals. *Phys. Rev. B* **78**, 153101 (2008).

[10] Notomi, M. Manipulating light with strongly modulated photonic crystals. *Rep. Prog. Phys.* **73**, 096501 (2010).

[11] Mortensen, N. A. & Xiao, S. Slow-light enhancement of beer-lambert-bouguer absorption. *Appl. Phys. Lett.* **90**, 141108 (2007).

[12] Jackson, J. *Classical electrodynamics* (Wiley, 1999).

[13] Boyd, R. *Nonlinear optics*. Academic Press (Academic Press, 2008).

[14] Agrawal, G. *Nonlinear Fiber Optics* (Academic Press, 2001), 4 edn.

[15] Joannopoulos, J. D., Johnson, S. G., Winn, J. N. & Meade, R. D. *Photonic Crystals: Molding the Flow of Light* (Princeton University Press, 2008), second edn.

[16] Sakoda, K. Optical properties of photonic crystals (2005).

[17] Kittel, C. *Introduction to Solid State Physics* (John Wiley & Sons, 2005).

[18] Ashcroft, N. & Mermin, N. *Solid state physics* (Holt, Rinehart and Winston, 1976).

[19] Toll, J. S. Causality and the dispersion relation: Logical foundations. *Phys. Rev.* **104**, 1760–1770 (1956).

[20] Milonni, P. *Fast light, slow light and left-handed light*. Series in optics and optoelectronics (Institute of Physics, 2005).

[21] Khurgin, J. B. Slow light in various media: a tutorial. *Adv. Opt. Photon.* **2**, 287–318 (2010).

[22] Boyd, R. & Gauthier, D. J. Controlling the velocity of light pulses. *Science* **326**, 1074 – 1077 (2009).

[23] Brillouin, L. *Wave propagation and group velocity* (1960).

[24] Buttiker, M. & Washburn, S. Optics - ado about nothing much? *Nature* **422**, 271–272 (2003).

[25] Veselago, V. G. Electrodynamics of substances with simulataneously negative values of ε and μ. *Sov. Phys. Uspekhi-USSR* **10**, 509 (1968).

[26] Boyd, R. Material slow light and structural slow light: Similarities and differences for nonlinear optics. *J. Opt. Soc. Am. B* (2011). In press.

[27] Stenner, M. D., Gauthier, D. J. & Neifeld, M. A. The speed of information in a 'fast-light' optical medium. *Nature* **425**, 695–698 (2003).

[28] Gehring, G. M., Schweinsberg, A., Barsi, C., Kostinski, N. & Boyd, R. W. Observation of backward pulse propagation through a medium with a negative group velocity. *Science* **312**, 895–897 (2006).

[29] Mørk, J. & Nielsen, T. R. On the use of slow light for enhancing waveguide properties. *Opt. Lett.* **35**, 2834–2836 (2010).

[30] Fleischhauer, M., Imamoglu, A. & Marangos, J. P. Electromagnetically induced transparency: Optics in coherent media. *Rev. Mod. Phys.* **77**, 633–673 (2005).

[31] Lukin, M. D. & Imamoglu, A. Controlling photons using electromagnetically induced transparency. *Nature* **413**, 273–276 (2001).

[32] Hau, L. Frozen light. *Sci. Am* **285**, 66–73 (2001).

[33] Kim, J., Chuang, S. L., Ku, P. C. & Chang-Hasnain, C. J. Slow light using semiconductor quantum dots. *Journal of Physics: Condensed Matter* **16** (2004).

[34] Mørk, J. *et al.* Slow and fast light in semiconductor waveguides. *Semicond. Sci. Technol.* **25** (2010).

[35] Mørk, J. *et al.* Slow and fast light: Controlling the speed of light using semiconductor waveguides. *Laser Photon. Rev.* **3**, 30 – 44 (2009).

[36] Nielsen, T. R., Lavrinenko, A. & Mørk, J. Slow light in quantum dot photonic crystal waveguides. *Appl. Phys. Lett.* **94**, 2009 (2009).

[37] Wu, B. *et al.* Slow light on a chip via atomic quantum state control. *Nat. Photonics* **4**, 776–779 (2010).

[38] Khurgin, J. & Tucker, R. *Slow light: science and applications*. Optical science and engineering (CRC Press, 2008).

[39] Yariv, A., Xu, Y., Lee, R. K. & Scherer, A. Coupled-resonator optical waveguide: a proposal and analysis. *Opt. Lett.* **24**, 711 – 713 (1999).

[40] Notomi, M., Kuramochi, E. & Tanabe, T. Large-scale arrays of ultrahigh-q coupled nanocavities. *Nature Phot.* **2**, 741–747 (2008).

[41] Altug, H. & Vuckovic, J. Experimental demonstration of the slow group velocity of light in two-dimensional coupled photonic crystal microcavity arrays. *Appl. Phys. Lett.* **86**, 111102 (2005).

[42] Mookherjea, S. & Yariv, A. Coupled resonator optical waveguides. *IEEE J. Sel. Top. Quantum Electron.* **8**, 448 – 456 (2002).

[43] Broaddus, D. H. *et al.* Silicon-waveguide-coupled high-q chalcogenide microspheres. *Opt. Express* **17**, 5998 – 6003 (2009).

[44] Morichetti, F., Ferrari, C., Canciamilla, A. & Melloni, A. The first decade of coupled resonator optical waveguides: bringing slow light to applications. *Laser Photonics Rev.* **6**, 74–96 (2012).

[45] Xia, L., F. Sekaric & Vlasov, Y. Ultracompact optical buffers on a silicon chip. *Nat. Photon.* **1** (2006).

[46] Cooper, M. L. *et al.* Statistics of light transport in 235-ring silicon coupled-resonator optical waveguides. *Opt. Express* **18**, 26505–26516 (2010).

[47] Poon, J. K. S., Chak, P., Choi, J. M. & Yariv, A. Slowing light with fabry-perot resonator arrays. *J. Opt. Soc. Am. B* **24**, 2763–2769 (2007).

[48] Scheuer, J., Paloczi, G. T., Poon, J. K. S. & Yariv, A. Coupled resonator optical waveguides: Toward the slowing and storage of light. *Opt. Photon. News* **16**, 36–40 (2005).

[49] Poon, J. K. S., Scheuer, J., Xu, Y. & Yariv, A. Designing coupled-resonator optical waveguide delay lines. *J. Opt. Soc. Am. B* **21**, 1665–1673 (2004).

[50] Melloni, A., Morichetti, F., Ferrari, C. & Martinelli, M. Continuously tunable 1 byte delay in coupled-resonator optical waveguides. *Opt. Lett.* **33**, 2389 – 2391 (2008).

[51] Poon, J. *et al.* Matrix analysis of microring coupled-resonator optical waveguides. *Opt. Express* **12**, 90–103 (2004).

[52] Johnson, S. G. & Joannopoulos, J. D. Block-iterative frequency-domain methods for maxwell's equations in a planewave basis. *Opt. Express* **8**, 173 – 190 (2001).

[53] Monat, C. *et al.* Slow light enhancement of nonlinear effects in silicon engineered photonic crystal waveguides. *Opt. Express* **17**, 2944–2953 (2009).

[54] Sakoda, K. Enhanced light amplification due to group-velocity anomaly peculiar to two- and three-dimensional photonic crystals. *Opt. Express* **4**, 167–176 (1999).

[55] John, S. Strong localization of photons in certain disordered dielectric superlattices. *Phys. Rev. Lett.* **58**, 2486–2489 (1987).

[56] Yablonovitch, E. Inhibited spontaneous emission in solid-state physics and electronics. *Phys. Rev. Lett.* **58**, 2059–2062 (1987).

[57] Cnrs, laboratory for photonics and nanostructures. URL `http://www.lpn.cnrs.fr/en/PHOTONIQ/SourcesCP.php`.

[58] SUSS-MicroTec. http://www.suss.com/markets/nanoimprint-lithography/scil.html .

[59] Lin, S. Y. *et al.* Athree-dimensional photonic crystal operating at infrared wavelengths. *Nature* **394** (1998).

[60] IBM-TJ. http://domino.research.ibm.com .

[61] Engelen, R. J. P. *et al.* The effect of higher-order dispersion on slow light propagation in photonic crystal waveguides. *Opt. Express* **14**, 1658 – 1672 (2006).

[62] Jensen, J. & Sigmund, O. Topology optimization for nano-photonics. *Laser Photon. Rev.* **5**, 308–321 (2011).

[63] Wang, F., Jensen, J. S. & Sigmund, O. Robust topology optimization of photonic crystal waveguides with tailored dispersion properties. *J. Opt. Soc. Am. B* **28**, 387–397 (2011).

[64] Dowling, J. P., Scalora, M., Bloemer, M. J. & Bowden, C. M. The photonic band edge laser: A new approach to gain enhancement. *J. Appl. Phys.* **75**, 1896 –1899 (1994).

[65] Busch, K. *et al.* Periodic nanostructures for photonics. *Phys. Rep.* **444**, 101 – 202 (2007).

[66] Knight, J. C. Photonic crystal fibres. *Nature* **424**, 847 – 851 (2003).

[67] Russell, P. S. Photonic-crystal fibers. *Lightwave Technology, Journal of* **24**, 4729–4749 (2006).

[68] Oskooi, A., Joannopoulos, J. & Johnson, S. Zero-group–velocity modes in chalcogenide holey photonic-crystal fibers. *Opt. Express* **17**, 10082–10090 (2009).

[69] Monat, C., de Sterke, M. & Eggleton, B. J. Slow light enhanced nonlinear optics in periodic structures. *J. Opt.* **12**, 104003 (2010).

[70] Mortensen, N. A., Xiao, S. S. & Pedersen, J. Liquid-infiltrated photonic crystals: enhanced light-matter interactions for lab-on-a-chip applications. *Microfluid. Nanofluid.* **4**, 117 – 127 (2008).

[71] Soljačić, M. & Joannopoulos, J. D. Enhancement of nonlinear effects using photonic crystals. *Nat. Mater.* **3**, 211 – 219 (2004).

[72] Corcoran, B. *et al.* Green light emission in silicon through slow-light enhanced third-harmonic generation in photonic-crystal waveguides. *Nat. Photon.* **3**, 206–210 (2009).

[73] Colman, P. *et al.* Temporal solitons and pulse compression in photonic crystal waveguides. *Nat. Photon.* **4**, 862 (2010).

[74] Soljačić, M. *et al.* Photonic-crystal slow-light enhancement of nonlinear phase sensitivity. *J. Opt. Soc. Am. B* **19**, 2052–2059 (2002).

[75] Bendickson, J. M., Dowling, J. P. & Scalora, M. Analytic expressions for the electromagnetic mode density in finite, one-dimensional, photonic band-gap structures. *Phys. Rev. E* **53** (1996).

[76] Martin, O. J. F., Girard, C., Smith, D. R. & Schultz, S. Generalized field propagator for arbitrary finite-size photonic band gap structures. *Phys. Rev. Lett.* **82**, 315–318 (1999).

[77] Gerace, D. & Andreani, L. C. Disorder-induced losses in photonic crystal waveguides with line defects. *Opt. Lett.* **29**, 1897–1899 (2004).

[78] Mazoyer, S., Hugonin, J. P. & Lalanne, P. Disorder-induced multiple scattering in photonic-crystal waveguides. *Phys. Rev. Lett.* **103**, 063903 (2009).

[79] Vlasov, Y. A., O'Boyle, M., Hamann, H. F. & Mcnab, S. J. Active control of slow light on a chip with photonic crystal waveguides. *Nature* **438**, 65 – 69 (2005).

[80] Notomi, M. *et al.* Extremely large group-velocity dispersion of line-defect waveguides in photonic crystal slabs. *Phys. Rev. Lett.* **87**, 253902 (2001).

[81] Martin, O. J. F., Girard, C. & Dereux, A. Generalized field propagator for electromagnetic scattering and light confinement. *Phys. Rev. Lett.* **74**, 526–529 (1995).

[82] McPhedran, R. C. *et al.* Density of states functions for photonic crystals. *Phys. Rev. E* **69**, 016609 (2004).

[83] Mortensen, N. A., Ejsing, S. & Xiao, S. Liquid-infiltrated photonic crystals: Ohmic dissipation and broadening of modes. *J. Europ. Opt. Soc. Rap. Public.* **1** (2006).

[84] Pedersen, J., Xiao, S. & Mortensen, N. A. Slow-light enhanced absorption for bio-chemical sensing applications: potential of low-contrast lossy materials. *J. Eur. Opt. Soc. Rap. Publ.* **3**, 08007 (2008).

[85] Johnson, S. G. *et al.* Perturbation theory for maxwell's equations with shifting material boundaries. *Phys. Rev. E* **65**, 066611 (2002).

[86] Fussell, D. P., Hughes, S. & Dignam, M. M. Influence of fabrication disorder on the optical properties of coupled-cavity photonic crystal waveguides. *Phys. Rev. B* **78**, 144201 (2008).

[87] Mookherjea, S. Spectral characteristics of coupled resonators. *J. Opt. Soc. Am. B* **23**, 1137 – 1145 (2006).

[88] Mookherjea, S. & Oh, A. Effect of disorder on slow light velocity in optical slow-wave structures. *Opt. Lett.* **32**, 289 – 291 (2007).

[89] Mookherjea, S., Park, J. S., Yang, S. H. & Bandaru, P. R. Localization in silicon nanophotonic slow-light waveguides. *Nature Photon.* **2**, 90 – 93 (2008).

[90] Anderson, P. W. Absence of diffusion in certain random lattices. *Phys. Rev.* **109**, 1492–1505 (1958).

[91] Datta, S. *Electronic Transport in Mesoscopic Systems* (Cambridge Studies in Semiconductor Physics Series, 1995).

[92] Datta, S. Nanoscale device simulation: The green's function formalism. *Superlattices Microstruct.* **28**, 253–278 (2000).

[93] Saitoh, K. & Koshiba, M. Leakage loss and group velocity dispersion in air-core photonic bandgap fibers. *Opt. Express* **11**, 3100–3109 (2003).

[94] Jensen, K. H., Alam, M. N., Scherer, B., Lambrecht, A. & Mortensen, N. A. Slow-light enhanced light-matter interactions with applications to gas sensing. *Opt. Commun.* **281**, 5335 (2008).

[95] Hamm, J. M., Wuestner, S., Tsakmakidis, K. L. & Hess, O. Theory of light amplifcation in active fishnet metamaterials. *Phys. Rev. Lett.* **107**, 167405 (2011).

[96] Stockman, M. I. Spaser action, loss compensation, and stability in plasmonic systems with gain. *Phys. Rev. Lett.* **106**, 156802 (2011).

[97] Li, D. B. & Ning, C. Z. Giant modal gain, amplified surface plasmon-polariton propagation, and slowing down of energy velocity in a metal-semiconductor-metal structure. *Phys. Rev. B* **80**, 153304 (2009).

[98] Mizuta, E., Watanabe, H. & Baba, T. All semiconductor low-delta. photonic crystal waveguide for semiconductor optical amplifier. *Jpn. J. Appl. Phys.* **45**, 6116–6120 (2006).

[99] Matsuo, S. *et al.* High-speed ultracompact buried heterostructure photonic-crystal laser with 13 fj of energy consumed per bit transmitted. *Nat. Photon.* **4**, 648–654 (2010).

[100] Agger, C., Skovg andrd, T., Gregersen, N. & M andrk, J. Modeling of mode-locked coupled-resonator optical waveguide lasers. *IEEE J. Quantum Electron.* **46**, 1804 –1812 (2010).

[101] Sukhorukov, A. & White, T. Slow light in photonic crystals with loss or gain. *Proc. SPIE* **7949**, 794903 (2011).

[102] Davanco, M., Urzhumov, Y. & Shvets, G. The complex bloch bands of a 2d plasmonic crystal displaying isotropic negative refraction. *Opt. Express* **15**, 9681–9691 (2007).

[103] Hughes, S., Ramunno, L., Young, J. F. & Sipe, J. E. Extrinsic optical scattering loss in photonic crystal waveguides: Role of fabrication disorder and photon group velocity. *Phys. Rev. Lett.* **94** (2005).

Included Papers

Paper A

J. Grgić, J. G. Pedersen, S. Xiao, and N. A. Mortensen

Group index limitations in slow-light photonic crystals

Photonics and Nanostructures - Fundamentals and Applications
8, 56 (2010)

Paper B

S. Raza, J. Grgić, J. G. Pedersen, S. Xiao and N. A. Mortensen

Coupled-resonator optical waveguides: Q-factor influence on slow-light propagation and the maximal group delay

J. Eur. Opt. Soc. Rap. Publ. 5, 10009 (2010)

Paper C

J. Grgić, E. Campagnoli, S. Raza, P. Bassi and N. A. Mortensen

Coupled-resonator optical waveguides: Q-factor and disorder influence

Opt. Quant. Electron. 42, 511 (2011)

Paper D

J. Grgić , S. Xiao, J. Mørk, A.-P. Jauho and N. A. Mortensen

Slow–light enhanced absorption in a hollow-core fiber

Opt. Express, 118, 14270–14279 (2010)

Paper E

J. Grgić, J. R. Ott, F. Wang, O. Sigmund, A.-P. Jauho, J. Mørk, and N. A. Mortensen

Fundamental limits to gain enhancement in periodic media and waveguides

Phys. Rev. Lett. **108**, 183903 (2012).